Large time behavior and asymptotic stability of the two-dimensional Euler and linearized Euler equations

Freddy Bouchet, Hidetoshi Morita

Large time behavior and asymptotic stability of the two-dimensional Euler and linearized Euler equations

Freddy Bouchet[+] and Hidetoshi Morita[+]

May 10, 2009

Affiliations : [+] INLN, CNRS, UNSA, 1361 route des lucioles, 06 560 Valbonne, France

Corresponding author : Freddy Bouchet ; email : Freddy.Bocuhet@inln.cnrs.fr

Keywords : 2D Euler equations, Large scales of turbulent flows, 2D turbulence, geophysical turbulence, asymptotic behavior, asymptotic Stability.

Abstract

We study the asymptotic behavior and the asymptotic stability of the two-dimensional Euler equations and of the two-dimensional linearized Euler equations close to parallel flows. We focus on spectrally stable jet profiles $U(y)$ with stationary streamlines y_0 such that $U'(y_0) = 0$, a case that has not been studied previously. We describe a new dynamical phenomenon: the depletion of the vorticity at the stationary streamlines. An unexpected consequence, is that the velocity decays for large times with power laws, similarly to what happens in the case of the Orr mechanism for base flows without stationary streamlines. The asymptotic behaviors of velocity and the asymptotic profiles of vorticity are theoretically predicted and compared with direct numerical simulations. We argue on the asymptotic stability of these flow velocities even in the absence of any dissipative mechanisms.

1 Introduction

The flow of a perfect fluid is described by the Euler equations, one of the oldest equations of mathematical physics [25]. Four century after their discovery by Euler, these equations still propose big challenges both to mathematician and physicists [25]. Two-dimensional flows and the two-dimensional Euler equations are mathematically much simpler than their three dimensional counterparts, but still present some very interesting unsolved problems. One of the main phenomena for two-dimensional flows is the self-organization of coherent structures [37, 45, 36, 55, 50, 35] : monopoles, dipoles, and parallel flows. Such large-scale structures are analogous to geophysical cyclones, anticyclones, and jets in the ocean and atmospheres. This analogy, understood thanks to the theoretical strong similarities between the 2D Euler equation on one hand and the Quasi-Geostrophic or the Shallow Water models on the other hand, is one of the main motivations for the study of the 2D Euler equations. The 2D Euler equation also describes experimental flows : the transverse dynamics of electron plasma columns [48], the dynamics of fluids when three-dimensional motion is prevented by a strong transverse field (rotation, a transverse magnetic field in a liquid metal, etc. [55],) or the dynamics of fluids in very thin geometries [43].

Because large-scale coherent flows appear spontaneously**,** their stability is a crucial problem. Moreover, the study of the dynamical mechanism close to such flows describes the relaxation to them. In this paper, we consider steady parallel base flows $\mathbf{v}_0(x,y) = U(y)\mathbf{e}_x$. We prove that these flow velocities are *asymptotically stable*[1], that is that all the solutions to the nonlinear Euler equations that start out near $\mathbf{v}_0$ converge to some other parallel flows $\mathbf{v}_0 + \delta U(y)\,\mathbf{e}_x$, close to $\mathbf{v}_0$. Our analysis mostly relies on the linearization of the Euler equation close to the base flows, which we prove to actually describe also the nonlinear relaxation. We quantitatively prove that the perturbation velocity decays algebraically. An important improvement over the previous works is the

[1]This convergence makes the notion of asymptotic stability stronger than the alternative Lyapounov stability, that state that all solutions of the nonlinear equations that start out near a steady point $\mathbf{v_0}$ stay near $\mathbf{v_0}$ forever. The asymptotic stability of the velocity refers to asymptotic stability in the kinetic energy norm.

understanding on the case when the velocity profile $U(y)$ has some stationary points y_0, $U'(y_0) = 0$, which has not been elucidated even qualitatively previously.

Besides the stability and the asymptotic stability problem itself, the evolution operator for the linearized Euler equation plays a very important role in different statistical approaches to turbulent flows [21, 18, 28]. Indeed, in a turbulent context, it is likely that the qualitative or quantitative properties of the fluctuations around such stable structures are related to the linearized dynamics. For instance, in quasi-linear approaches or second order closure of the evolution of the Euler equations, point vortex model [21], or of the Navier-Stokes equation (either forced or unforced, and either deterministic or stochastic,) the linear operator appears naturally as an essential theoretical tool. Similarly, in the forced problems, in the linear regime, the response can be easily expressed in terms of the evolution operator for the linearized dynamics or of the resolvent operator for the dynamics. The behavior of such operators for large times is thus a very important issue that has many theoretical and dynamical consequences. In this work, we quantify very precisely the large time asymptotic behavior of the evolution operator for the linearized 2D-Euler equations, and discuss briefly some of the implications for the above problems.

The stability of the large-scale coherent structures of two-dimensional flows is a very old and classical field of fluid mechanics. For instance Rayleigh [44], Kelvin [56], Orr [42], Sommerfeld [54] and many other famous scientists from the nineteenth and the beginning of the twentieth century have participated to the understanding of the linear theory for the 2D Euler equations close to parallel flows. Mathematicians gave also important contributions : Arnold's theorems [2] and some modern generalizations [60, 52, 23, 16, 9] prove the Lyapounov stability of some of these flows ; recently many works have been devoted to the proof of the instability of some classes of flows, the characterization of the spectrum of the linearized equations, and some estimates on the stability and the instability of such flows; see for instance [29, 51, 30] and references therein.

Our work is based on the linearized 2D Euler equations. The Rayleigh equation [44], which describes modes for the linear dynamics, has been a subject of mathematical and theoretical research since the beginning of the twentieth century [20], and is still currently active. The main interest lies in the dynamical phenomena associated with the singularities at the critical layers (the singularities appearing when the frequency of the perturbation is equal to that of a closed streamline of the base flow). However, the modes of the Rayleigh equation do not describe the fully linearized dynamics, because the linear operator is non-normal [27]. Among the peculiarities of the linearized Euler equations, we stress the Orr mechanism [42]: the base flow shears the perturbation producing thinner and thinner filaments ; then when the velocity or the streamfunction is computed, the effect of such filaments being smoothed out, the perturbation velocity decays for large times. This mechanism is easily quantified when the shear is linear [42], or using for instance Kelvin waves [56] for viscous flows. Case [17] and Dikii [19] were the first to stress that in general, for inviscid flows, such a phenomenon is outside the scope of a modal description using the Rayleigh equation. When the shear is linear, using a Fourier-Laplace transform, the dynamics of the perturbation is properly described in the framework of an initial value problems. They concluded that the perturbation velocity decreases asymptotically with an algebraic law for large times. Other phenomena associated to the non-normality of the linear operator include possible transient growth [26, 59, 1], inviscid damping (the counterpart of Landau damping in plasmas), axisymmetrization [47, 33], and algebraic instabilities [41]. From a mathematical point of view, the singularities at the critical layers lead to the existence of a continuous spectrum for the linearized Euler equation. The analysis of the properties of this continuous spectrum explains most of these transient growth, inviscid damping, algebraic instabilities, and so on.

From a theoretical point of view, one class of works used the Laplace transform tools [4, 48], following the initial works of Case [17], Dikii [19] and the generalization to non-uniform shear by Briggs-Daugherty and Levy [11]. Another class of studies, less general but very enlightening, used simple or particular base flows or special conditions for which explicit computations are possible [56, 42, 61, 26, 57, 13, 14, 15, 41].

In this paper, we are especially interested in the precise description of the large time asymptotic behavior of the 2D Euler and 2D linearized Euler equation close to the parallel base flows. For stable base flows, once the contribution of possible neutral modes has been subtracted, the asymptotic behavior is related to the continuous spectrum of the linearized operator. In the case of the base flow with a linear shear, $U(y) = \sigma y$, the explicit computations by Case [17] showed that, due to the Orr mechanism, for large times the velocity perturbation decays algebraically :

$$v_x \underset{t\to\infty}{\sim} \frac{C(y)}{t^\alpha} \text{ and } v_y \underset{t\to\infty}{\sim} \frac{C(y)}{t^\beta}, \tag{1}$$

with exponents $\alpha = 1$ for the longitudinal component v_x of the velocity perturbation and $\beta = 2$ for the transverse one v_y. For more general base flows with strictly monotonic profiles $U(y)$ (without stationary streamline), from classical arguments [46, 11] using the Laplace transform, we conclude that the contribution

of the continuous spectrum to the stream function perturbation ψ and the transverse velocity perturbation v_y decays with $\psi \underset{t\to\infty}{=} \mathcal{O}\left(\frac{1}{t}\right)$ and $v_y \underset{t\to\infty}{=} \mathcal{O}\left(\frac{1}{t}\right)$. Except for the case of a linear shear cited above [17], we have found no proofs in the literature for the exact values of the exponents α and β. It is however a common belief that the exponents $\alpha = 1$ and $\beta = 2$ remain valid in the case of a monotonic profile. This belief is based on the results of an ansatz for large time asymptotics [12] (see also [34], appendix A). In the case of a circular vortex base flow, we refer to [7], where the far field velocity is shown to decay with other exponents.

From Lundgren work ([34], appendix A), we see that the preceding algebraic decay for the velocity may be related to the following asymptotic behavior for the perturbation vorticity :

$$\omega(y,t) \underset{t\to\infty}{\sim} \omega_\infty(y) \exp(-ikU(y)t) + \mathcal{O}\left(\frac{1}{t^\gamma}\right), \tag{2}$$

where k is the initial perturbation wave number. Indeed, computing the velocity from Lundgren's ansatz (equation (2)) and assuming uniformity in the asymptotic expansion, we obtain oscillating integrals leading to algebraic decay for large times. The values for the exponents $\alpha = 1$ and $\beta = 2$ are then related to the singularities of the Green function used in order to compute the vorticity perturbation from the velocity perturbation. This argument, assuming Lundgren's ansatz, suggest that the asymptotic behavior for the velocity should be different for velocity profiles $U(y)$ with stationary points y_0 ($U'(y_0) = 0$). Actually, in such a case, the stationary phase approximation of oscillating integrals would generically give $1/\sqrt{t}$ contributions. It has been noticed by several authors, that Lundgren's ansatz does not seem to be self-consistent in such a case [12, 15, 13]. This has also been noticed by Brown and Stewartson [12], as their ansatz clearly breaks down where $U'(y) = 0$. Besides Lundgren and Stewartson, many authors have insisted on the specificity of base flow profiles with stationary point (see for instance [15, 13, 31]). The asymptotic behavior of the vorticity and velocity perturbations of this last case remains unstudied. This is an important problem, as the decay exponents for the velocity perturbation plays a crucial role in kinetic theories, or quasi-linear theories or closure approaches to two-dimensional flows, as discussed above.

Most of the previous works have studied only monotonic velocity profiles $U(y)$ for parallel flows and monotonic angular velocity profiles $U(r)/r$ for circular vortices $\mathbf{v}(r) = U(r)\,\mathbf{e}_\theta$. In natural flows, however, the velocity profiles of jets are usually not monotonic but have some extrema, i.e. stationary points y_0 such that $U'(y_0) = 0$ [2]; for instance, Jupiter, atmospheric, and ocean jets. Why the case with stationary points have not studied? This may be partially on account of the wrong belief that base velocity profiles with stationary points should be unstable. It is true that they do not fulfill the classical Rayleigh-Fjørtoft criteria [20]. However, these criteria are only sufficient conditions of stability; as seen in natural flows and shown bellow with several examples, many parallel flows with stationary points in their velocity profile are actually stable. That may be also due to the theoretical difficulty with Laplace tools, related to the presence of stationary points (merging of critical layers). Indeed, an essential tool for the Laplace transform is the analytic continuation of dynamical quantities, performed by avoiding the singularities associated to the critical layers, with the use of integration in the complex plane for the spatial variable [20]. As will be discussed bellow, in the case of flows with stationary points, one would need to pass both above and bellow the singularity at the same time, and such a procedure is impossible. For this reason, it has often been stated that Laplace tools cannot be used in such a case. By contrast, we illustrate in this work that even if analytic continuation can not been performed in this way, Laplace tools are still very useful and lead to very interesting results.

In the past, there have been only a few studies considering base velocity profiles with stationary points. In the case of the equations for 2D barotropic flows on a β plane (a direct generalization of the 2D Euler equations), Brunet and coauthors [15, 13] have studied the dynamics close to a parabolic jet when the vorticity gradient exactly cancels the β effect. This case is similar to the linear shear case in the Euler equations studied by Kelvin, Orr, Case and others [56, 42, 17, 57, 26], in that the vorticity gradient exactly cancels out, which makes the linearized equation much simpler and amenable to an explicit analytic treatment. In the following, we will argue that, because of the cancellation of the vorticity gradient, the dynamics of these cases is actually non generic. For circular vortex base flows, an example of non-monotonic angular velocity profile has been studied [41], based on a special explicit solution [53]. This example shows a very interesting algebraic instability with $t^{1/2}$ growths. In the following we will consider the generic case of a parallel flow with any profile, either with or without stationary points, improving by far the class of studied flows. We will also discuss possible generalizations to monopole vortices.

[2] These are stationary points of the profile, not of the flow itself

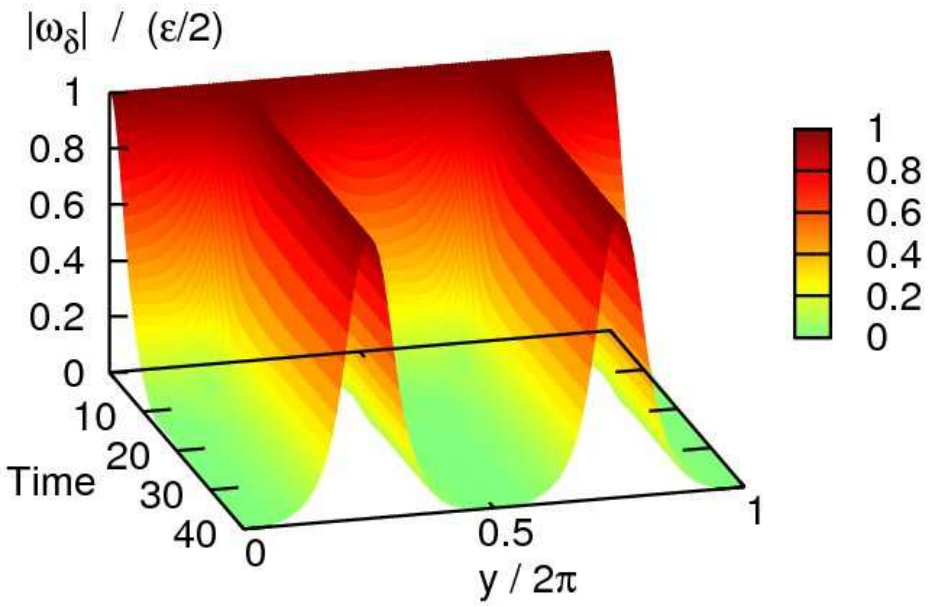

Figure 1: Evolution of the vorticity perturbation $\omega(x,y,t) = \omega(y,t)\exp(ikx)$, close to a parallel flow $\mathbf{v}_0(x,y) = U(y)\mathbf{e}_x$ with $U(y) = \cos(y)$. The figure shows the modulus of the perturbation $|\omega(y,t)|$ as a function of time and y. One clearly sees that the vorticity perturbation rapidly converges to zero close to the points where the velocity profile $U(y)$ has extrema ($y = 0$ and π). This *perturbation vorticity depletion* is a new generic self-consistent mechanism, understood mathematically as the regularization of the critical layer singularities at the edge of the continuous spectrum.

In this paper, we show how the Laplace transform is generalized to the case of base flow with stationary points. For instance, we show how the classical determination of the number of unstable modes, by using Nyquist's plots, remains valid in this case. From this general theoretical approach, we prove that the asymptotic vorticity field actually follows the Lundgren's ansatz (2), even in the case of a base profile with stationary points. Similarly the velocity field decreases also algebraically with the power laws (1), with $\alpha = 1$ and $\beta = 2$[3]. This may seem paradoxical, after the discussion of the preceding paragraphs. Indeed, the naturally expected $1/\sqrt{t}$ contributions from the stationary phase arguments do not exist. One reason is the non-uniformity of the asymptotic expansion in Lundgren's ansatz. Another more important reason is related to a new dynamical phenomena leading to the rapid decrease and cancellation of the vorticity perturbation exactly at the stationary points (see Fig. 1), which partially erase the effect of the stationary phase. We call this phenomena *vorticity depletion at the stationary streamlines*. This is a non-local collective phenomena, due to the effect of the perturbation velocity on the background vorticity gradient. For this reason, this phenomena has not been observed in the previous studies of base profile with stationary points [15, 13, 31]), in the non-generic case when the total vorticity of the base flow exactly cancels.

In the following, we predict the vorticity depletion at the stationary streamlines using Laplace tools. It is thus a generic effect in any type of non-monotonic stable base flows. We also illustrate the results by direct numerical simulations in the case of Kolmogorov base flow $U(y) = \cos y$, for the 2D Euler equations with periodic boundary conditions. Even if we do not explicitly treat the case of stable circular vortices $\mathbf{v}(r) = U(r)\,\mathbf{e}_\theta$ in the present study, the generalization to this case could be taken following similar theoretical arguments as discussed in the conclusion. This vorticity depletion mechanism also impacts turbulent flows where the perturbations are locally governed by the linearized equations, as discussed in the conclusion.

Having established the large time asymptotic contributions, by the continuous spectrum, to the vorticity (2) and to the velocity fields (1), we are able to discuss the asymptotic stability of the velocity of parallel base flow. The result is that parallel base flows which have no mode (neither stable nor unstable) are asymptotically stable : any small perturbation leads to a small deformation of the base flow, the perturbation velocity to this new base flow decaying algebraically. Stable Kolmogorov flows are examples of base flows without modes, illustrating the importance of this class of flows.

[3] An exception is the velocity field close to the stationary streamline, where we have no theoretical prediction, but where we observe numerically that either $\alpha = 1$ and $\beta = 2$ or $\alpha = \beta = 3/2$ depending on the symmetry of the perturbation.

In section 2 we introduce the 2D Euler equation and the linearized Euler equation. Section 2 describes the theory related to the linearized Euler equation. We discuss the main results about the asymptotic behavior of the vorticity and velocity fields in section 2.2. The core of the proof relies on the results of the analysis on the limit of small ϵ for the resolvent operator in section 2.3.

These results are illustrated in the case of doubly periodic boundary conditions, with the Kolmogorov flows as a base flow, in section 4. For some aspect ratio, these flow are stable even if they do not fulfill the hypothesis of any of the two Arnold's theorems. Applying Arnold's ideas to this case, we first prove their Lyapounov stability in section 4.1. In section 4.3, we show the results of direct numerical simulations of the 2D Euler equations (nonlinear), which both illustrate the theoretical results of section 2, and show that the linearized dynamics correctly describes the nonlinear one.

Section 3 discusses the asymptotic stability of parallel flows for the Euler equation. Section 5 discusses briefly some consequences of these results for the 2D Euler and Navier-Stokes equations with stochastic forces and for possible theories relying on a quasi-linear or kinetic approach. It also discusses some possible generalizations to models of interest for geophysical flows.

2 The 2D Euler and linearized Euler equations

Let us consider the Euler equations

$$\frac{\partial \Omega}{\partial t} + \mathbf{V}.\nabla\Omega = 0, \tag{3}$$

where Ω is the vorticity and $\mathbf{V}$ is the velocity. We consider this equation either in an infinite plane, in a channel geometry with boundary conditions $\mathbf{V}.\mathbf{n} = 0$ on the boundary wall, or on a doubly periodic domain $(0, 2\pi/\delta)\,(0, 2\pi)$, where $\delta > 1$ is the aspect ratio. In some parts of the discussion, for technical reasons the boundary conditions will be important. Then only the case of a doubly periodic domain will be explicitly treated. However all the results are applicable to the channel and infinite domain geometries.

We study the asymptotic stability of parallel flows $\mathbf{v}_0{=}U(y)\,\mathbf{e}_x$. We will thus consider the Euler equations (3) with initial conditions close to this base flow : $\Omega = \omega_0 + \omega$ and $\mathbf{V} = \mathbf{v} + \mathbf{v}_0$, where $\omega_0(y) = -U'(y)$ is the base flow vorticity and ω and $\mathbf{v}$ are the perturbation vorticity and velocity, respectively.

We also need to consider the linearized Euler equation close to this base flow. It reads

$$\frac{\partial \omega}{\partial t} + \mathbf{v}.\nabla\omega_0 + \mathbf{v}_0.\nabla\omega = 0. \tag{4}$$

We assume that the base flow $U(y)$ has no unstable mode (a precise definition of modes will be given along the discussion). In section 4 we will illustrate some of the results on the particular case of the Kolmogorov flow $U(y) = \cos y$ (in a doubly periodic domain).

2.1 The Laplace transform, resolvent operator and Rayleigh equation

In this section and the following we consider the linearized Euler equation. We give the main definitions used later on in the discussion.

We decompose the perturbation vorticity in Fourier series for the x variable only. For parallel flows, due to the translational invariance, these Fourier modes are independent one from the others for the linear dynamics. In the following, we thus study perturbations of the form $\omega(x, y, t) = \omega_k(y, t)\exp(ikx)$ and $\psi(x, y, t) = \psi_k(y, t)\exp(ikx)$, where ψ is the stream function, with $\omega = \Delta\psi$ and k is the longitudinal wave number. In the following, we drop the k subscripts for the perturbation. The relations between ω, $\mathbf{v}$ and ψ are then

$$\omega = \frac{d^2\psi}{dy^2} - k^2\psi, \;\; v_x = -\frac{d\psi}{dy} \text{ and } v_y = ik\psi. \tag{5}$$

The linearized Euler equations then reads

$$\frac{\partial \omega}{\partial t} + ikU(y)\,\omega - ik\psi U''(y) = 0, \tag{6}$$

We will study the long time asymptotics of the linearized equation. The more general approach is to use the Laplace transform of equation (6). We define the Laplace transform $\hat{\omega}$ of ω as

$$\hat{\omega}(y,p) = \int_0^\infty dt\, \omega(y,t) \exp(-pt)$$

The Laplace transform is analytic for any complex number p for sufficiently large real part $\Re p$. The inverse Laplace transform is given by

$$\omega(y,t) = \frac{1}{2\pi i} \int_\Gamma dp\, \hat{\omega}(y,p) \exp(pt) \tag{7}$$

where the complex integration is performed along a Bromwich contour Γ in the complex plane of p. In the following we use the notation $p = -ik(c + i\epsilon)$ where c and ϵ are real numbers ; c and ϵ are homogeneous to velocities. We assume $k > 0$. The Laplace transform $\hat{\omega}$ is thus analytic for sufficiently large ϵ.

The Laplace transform of equation (6) reads

$$(U(y) - c - i\epsilon)\,\hat{\omega} - U''(y)\,\phi = \frac{\omega(y,0)}{ik}, \tag{8}$$

where $\phi = \hat{\psi}$ is the Laplace transform of ψ and $\omega(y,0)$ is the initial value for the vorticity field. We have

$$\hat{\omega} = \frac{d^2\phi}{dy^2} - k^2\phi$$

From a mathematical point of view, we have to solve the equation for ϕ

$$\left(\frac{d^2}{dy^2} - k^2\right)\phi - \frac{U''}{U - c - i\epsilon}\phi = \frac{\omega(y,0)}{ik(U - c - i\epsilon)}, \tag{9}$$

with the boundary condition for ϕ (here ϕ doubly periodic). The solution of this boundary value problem $\phi[\omega(.,0)](y, c + i\epsilon)$ depends functionally on the initial value of the vorticity $\omega(y,0)$ (ϕ is the resolvent operator for the stream function). This resolvent operator encodes all the information about the temporal evolution of the stream function and the vorticity field.

The homogeneous part of equation (9) is the celebrated Rayleigh equation. It is also the equation for modes ($\psi = \phi(y) \exp[ik(x - (c + i\epsilon)t)]$) of the linearized Euler equation (4). It reads

$$\left(\frac{d^2}{dy^2} - k^2\right)\phi - \frac{U''}{U - c - i\epsilon}\phi = 0, \tag{10}$$

with the flow boundary conditions. For neutral modes ($\epsilon = 0$), this is a non-classical boundary value problem, because of the possible singularities associated to the vanishing of $U - c$. Any y_c such that $U(y_c) = c$ is called a critical point for the velocity c. For any c, the free motion on the streamline $y = y_c$ is called the critical layer and has exactly the frequency kc.

Any y_0 such that $U'(y_0) = 0$ (no shear, for instance for velocity extrema) is called a stationary point of the jet profile, corresponding to a stationary streamline. We then call $c_0 = U(y_0)$ a stationary velocity. If y_0 is a local extrema of U, we note that when $y \to y_0$ (or equivalently $c \to c_0 = U(y_0)$), two critical layers, one on each side of the velocity extrema, merge on a single one.

The range of the profile U is the ensemble of velocities c such that $\min_y U(y) < c < \max_y U(y)$.

In the following we assume that the base flow is spectrally stable, i.e., no unstable mode exist, which means that no solution to (10) exist for any $c + i\epsilon$ with strictly positive $\epsilon > 0$. Then, as shown in section 2.3, equation (9) has a unique solution for any $c + i\epsilon$ with strictly positive $\epsilon > 0$. We also assume that no neutral mode exist, which means that no solutions to (10) is found in the limit $\epsilon \to 0^+$(a more precise definition will be given bellow in terms of the dispersion relation). This no mode assumption for equation (6) may seem strange, but it is indeed a generic situation when such flows are stables. For instance, in section 4, we prove that this hypothesis is verified for the Kolmogorov flow $U(y) = \cos(y)$ as soon as the aspect ratio δ is larger than 1.

The case where neutral modes exist could be treated following the same lines as what will be discussed bellow ; one would then have to separate the contributions by the neutral modes from the contributions by the continuous spectrum. The following discussion analyzes the contributions by the continuous spectrum only.

2.2 Large time asymptotic for the linearized Euler equation

In this section, we predict the large time asymptotic of the linearized Euler equation, using Laplace transform tools. We prove results (1) and (2) and the mechanism of vorticity depletion at stationary streamlines. The heart of the proof relies on the study of the effect of critical layers, on the inhomogeneous Rayleigh equation (9), in the limit ϵ goes to zero. This rather technical part is performed in section (2.3).

The results of section (2.3) are that the resolvent streamfunction ϕ, solution of (9), has a finite limit for small positive ϵ :

$$\phi\left(y, c+i\epsilon\right) \underset{\epsilon\to 0^+}{\to} \phi_+\left(y, c\right), \tag{11}$$

even if singularities exist due to the critical layers. We prove that for any y, $\phi_+\left(y, c\right)$ is twice differentiable with respect to c, except for velocities c that are in the interior of the range of U. In this last case, for velocities c that are not stationary, ϕ_+ is twice differentiable, except only for $c = U\left(y\right)$, where ϕ_+ is continuous but not differentiable there, and has a logarithmic singularity : for fixed y $\phi_+\left(y, c\right) = \Delta\phi_c\left(c - U\left(y\right)\right)\log\left(c - U\left(y\right)\right) + R\left(y, c\right)$, where $R\left(y, .\right)$ is an analytic function of c. When $c = c_0$ is a stationary velocity, $\phi_+\left(y, c_0\right)$ is differentiable with respect to c.

We think that all of the steps of these proofs could be easily made rigorous from a mathematical point of view, by making explicit the required hypothesis. An exception is for the limit of ϕ in the case of critical layers for stationary points. We actually prove in the following that a limit solution exist for $\epsilon = 0$, but we do not prove the convergence to it when $\epsilon \to 0$. In order to deal with this small gap in the proof, we will show, by numerically computing $\phi\left(y, \epsilon\right)$, that this convergence actually takes place.

These results (the limit and its properties) are the difficult aspects of the discussion, from a mathematical point of view. Their technical proof can be skipped at a first reading, the next sections can be read independently by assuming these results. The discussion then follows by performing the inverse Laplace transform and proving results (1) and (2) in sections 2.3.4 and 2.3.5.

2.3 Limit for $\epsilon \to 0^+$ of the resolvent operator

2.3.1 The dispersion relation

The equation defining the resolvent operator for the stream function (9) is of the type

$$\frac{d^2\phi}{dy^2} + q(y)\phi = f(y) \tag{12}$$

with $q = -k^2 - U''/(U - c - i\epsilon)$ and $f = \omega(y, 0)/ik/(U - c - i\epsilon)$. This is a boundary value problem. In order to be precise, we treat the case of a doubly periodic domain with the period 2π, although that is easily generalized to the case of a flow in a channel $y \in (a, b)$ with the boundary conditions $\phi(a) = \phi(b) = 0$.

For $\epsilon \neq 0$, the differential equation is not singular. We consider the homogeneous equation

$$\frac{d^2\phi}{dy^2} + q(y)\phi = 0. \tag{13}$$

We consider two independent solutions to (13) : ϕ_1 is defined by $\phi_1\left(0\right) = 1$ and $\phi_1'\left(0\right) = 0$, and ϕ_2 is defined by $\phi_2\left(0\right) = 0$ and $\phi_2' = 1$ (here and bellow, primes are derivatives with respect to y). The classical variation of the parameter then insures that a particular solution to (12) is

$$\phi_p\left(y\right) = -\left(\int_0^y \phi_2 f\right)\phi_1\left(y\right) + \left(\int_0^y \phi_1 f\right)\phi_2\left(y\right),$$

and a general solution is

$$\phi_f = \phi_p + a\phi_1 + b\phi_2, \tag{14}$$

where a and b are unknown constants. The necessary and sufficient conditions for ϕ to be periodic are that $\phi(0) = \phi\left(2\pi\right)$ and $\phi'(0) = \phi'\left(2\pi\right)$. These conditions read

$$M\begin{pmatrix} a \\ b \end{pmatrix} = \begin{pmatrix} -\phi_p\left(2\pi\right) \\ -\phi_p'\left(2\pi\right) \end{pmatrix} \text{ with } M = \begin{pmatrix} \phi_1\left(2\pi\right) - 1 & \phi_2\left(2\pi\right) \\ \phi_1'\left(2\pi\right) & \phi_2'\left(2\pi\right) - 1 \end{pmatrix} \tag{15}$$

This system has a single solution if and only if the determinant of M is nonzero, which gives the dispersion relation

$$D\left(c+i\epsilon\right) \equiv \left[\phi_1\left(2\pi\right)-1\right]\left[\phi_2'\left(2\pi\right)-1\right] - \phi_1'\left(2\pi\right)\phi_2\left(2\pi\right) = 0. \tag{16}$$

The existence of modes (nontrivial solutions to (13)) is then equivalent to the zero values of the dispersion relations. When no mode exist, D is nonzero and (12) has thus a unique periodic solution ϕ_f (14), with a and b the unique solution to (15).

Turning back to the inhomogeneous Rayleigh equation, the preceding discussion applies as soon as $\epsilon \neq 0$. We assume that no unstable mode exists, then $D\left(c+i\epsilon\right)$ is nonzero. Then the inhomogeneous Rayleigh equation has a unique solution for any $c+i\epsilon$, for nonzero ϵ.

The limit $\epsilon \to 0$ of $\phi_f\left(c+i\epsilon\right)$ is nontrivial due to the existence of critical layers $y_c\left(c\right)$, for which the Rayleigh equation becomes singular. We study this limit in the following sections.

2.3.2 Limit $\epsilon \to 0^+$ for isolated critical layers

We consider fixed values of c which are on the range of U : $\min_y\left\{U\left(y\right)\right\} < c < \max_y\left\{U\left(y\right)\right\}$. In such a case, for any value of c, there exist one or several points y_l such that $U(y_l) = c$. The inhomogeneous Rayleigh equation is then singular at such critical layers. We discuss in this section the case $U'(y_l) \neq 0$ (isolated critical layers). The case $U'(y_l) = 0$ will be treated in the next section.

In order to properly study the limit $\epsilon \to 0$, we first build a solution to the homogeneous equation (10), which is regular at one of the critical layers $y = y_l$. We define $\phi_r\left(y,c\right)$ as the solution to (10) with $\phi_r\left(y_l,c\right) = 0$ and $\phi_r'\left(y_l,c\right) = 1$. From (10), we have $\phi_r''\left(y_l,c\right) = U''(y_l)/U'(y_c)$. We then have the expansion

$$\phi_r\left(y,c\right) = \left(y-y_l\left(c\right)\right)\left[1+\frac{U''\left(y_l\left(c\right)\right)}{2U'\left(y_l\left(c\right)\right)}\left(y-y_l\left(c\right)\right)+o\left(y-y_l\right)\right] \tag{17}$$

It can be shown that the solution $\phi_r\left(y,c\right)$ is an analytic function of y in the vicinity of y_l, if we suppose that $U\left(y\right)$ is analytic in a vicinity of y_l. Moreover, from the definition $U\left(y_l\left(c\right)\right) = c$, because $U'\left(y_l\right) \neq 0$, then $y_l\left(c\right)$ is analytic in a vicinity of c and $dy_l/dc = 1/U'\left(y_l\right)$. The solution $\phi_r\left(y,c'\right)$ has then an analytic continuation for complex c' in the vicinity of c.

A classical result of the theory of differential equation of second order is that, if we already know a solution ϕ_r, all other solutions ϕ is expressed in terms of ϕ_r by quadratures. The recipe for this is to look for solutions under the form $\phi = u\phi_r$, look for the equation verified by u and integrate it. We apply this recipe to the inhomogeneous Rayleigh equation (9). Then any solution ϕ to (9) is expressed as

$$\phi(y) = d\phi_r(y) + \phi_r(y)\int_{y_0}^{y}\frac{(e+f)}{\phi_r^2} \quad \text{with} \tag{18}$$

$$f(y) = \int_{y_0}^{y} dy_2\,\frac{\omega\left(y_2,0\right)\phi_r(y_2)}{ik\left(U(y_2)-c-i\epsilon\right)},$$

and where d and e are constants.

We study the behavior of the previous expression close to y_l. We first note that f is analytic close to y_l. Then using the expansion (17), we conclude that

$$\phi(y,c+i\epsilon) = d\phi_r(y,c+i\epsilon) + g\phi_r(y,c+i\epsilon)\log\left(y-y_l(c+i\epsilon)\right) + e\phi_g\left(y,c+i\epsilon\right) + \phi_h\left(y,c+i\epsilon\right) \tag{19}$$

where ϕ_g and ϕ_h are analytic functions of y close to y_l, and where g is a constant that depends on $f(y_l)$, $f'\left(y_l\right)$ and e.

The interpretation of (19) depends on which determination of the logarithm we use. Using $dy_l/dc = 1/U'\left(y_l\right)$ (discussed above), we have $y_l\left(c+i\epsilon\right) = y_l\left(c\right) + i\epsilon/U'\left(y_l\right) + o\left(\epsilon\right)$. We choose a determination of the logarithm such that $\log\left(y-y_l(c)-i\epsilon/U'\left(y_l\right)\right)$ remains analytic for positive ϵ. Then the study of the limit $\epsilon \to 0$ of equation (14) is easily done, we denote this limit $\phi\left(y,c+i0\right)$. Using that ϕ_r and ϕ_g depends analytically on c, we obtain

$$\phi(y,c+i0) = d\phi_r(y,c) + g\phi_r(y,c)\log|y-y_l| + e\phi_g\left(y,c\right) + \phi_h\left(y,c\right) \;\text{ for }\; y > y_l \;\text{ and} \tag{20}$$

$$\phi(y, c+i0) = (d - i\pi \mathrm{sgn}\,(U'(y_l))\, g)\phi_r(y,c) + g\phi_r(y,c)\log|y-y_l| + e\phi_g\,(y,c) + \phi_h\,(y,c) \quad \text{for } y < y_l \tag{21}$$

where $\mathrm{sgn}\,(U'(y_l))$ is the sign of $U'(y_l)$.

From this, we conclude that, for given d and e, the solution to the inhomogeneous Rayleigh equation (9) converges, for $\epsilon \to 0$, towards a function $\phi\,(y, c+i0)$, which is an analytical function of y, except for $y = y_l$ where it has a logarithmic singularity. It is continuous at $y = y_l$. This result is valid close to a single layer y_l. If two or several critical layer $y_{l,i}$ exist in the interval $y \in (0, 2\pi)$, then the result is easily extended, and holds with a singularity at each critical layer.

Is this result also true for the solution $\phi_\omega(y, c+i\epsilon)$ of the inhomogeneous Rayleigh equation with boundary conditions ? In order to answer this, we now turn again to the construction of section 2.3.1. The result of the previous paragraph is applied alternatively to $\phi_1(y, c+i\epsilon)$, $\phi_2\,(y, c+i\epsilon)$ and to $\phi_p(y, c+i\epsilon)$. We thus conclude that all these three functions have well-defined limits for $\epsilon \to 0^+$, and that these limits are continuous functions of y, which have logarithmic singularities in their derivative for each critical layer. We can then extent the definition of the dispersion relation to $\epsilon \to 0^+$ with $D_+\,(c) = \lim_{\epsilon\to 0^+} D\,(c+i\epsilon)$. $D_+\,(c)$ verifies (16) for which we have proved that all terms have a finite limit when $\epsilon \to 0^+$. Then we conclude that the two parameters a and b in equation (14) have finite limits when $\epsilon \to 0^+$. These limit values are given by equation (15), where each term has a finite limit.

We thus conclude that the solution to the Rayleigh equation with boundary conditions $\phi_\omega(y, c+i\epsilon)$ has a finite limit $\phi_+\,(y, c)$ for $\epsilon \to 0^+$. Moreover, $\phi_+\,(y, c)$ is a continuous function of y that has a logarithmic singularity at each critical layer, giving a finite jump for the first derivative.

Let us denote $\Delta\phi_+$ this jump. From the previous analysis we know that

$$\phi_+\,(y, c) = a + b\,(y - y_l) + \Delta\phi_+(y - y_l)\log|y - y_l| + \mathcal{O}\,(y - y_l)^2 \tag{22}$$

Using this expansion, a direct analysis of the dominant term in (9) leads to

$$\Delta\phi_+ = \frac{\omega\,(y_l, 0) + ikU''\,(y_l)\,\phi_+\,(y_l, c)}{ikU'\,(y_l)}.$$

The jump in the derivative thus depends on the value of ϕ_+ which is a non local quantity (ϕ_+ depends on the whole profile U).

Because ϕ_r and y_l are analytic functions of c, the construction of ϕ_+ can be extended analytically when c is varied. Then from (22), using $y_l\,(c') = y_l\,(c) + (c' - c)/U'(y_l)$, one sees that, for fixed y :

$$\phi_+\,(y, c) = \Delta\phi_c\,(U\,(y) - c)\log\,(U\,(y) - c) + \phi_a\,(y, c)\,, \tag{23}$$

where $\phi_a\,(y, c)$ is analytic close to $c = U\,(y)$ and with

$$\Delta\phi_c = \frac{\Delta\phi_+}{U'\,(y)} = \frac{\omega\,(y, 0) + ikU''\,(y)\,\phi_+\,(y, U\,(y))}{ik\,(U'\,(y))^2} \tag{24}$$

We illustrate the preceding results with numerical solutions of the inhomogeneous Rayleigh equations on a doubly periodic domain, and the base flow $U\,(y) = \cos y$ (the Kolmogorov flow).

We follow the algorithm described in section 2.3.1, that is, computing ϕ_1, ϕ_2, and ϕ_p, and then by using them, computing the solution to the inhomogeneous Rayleigh equation for $c' = c + i\epsilon$ for small but nonzero value of ϵ. In order to numerically compute the solution to the differential equations (for ϕ_1, ϕ_2, and ϕ_p), we use an adaptive method to deal with the singularity close to the critical layers. An extreme precision is required in order to obtain satisfactory results.

In order to test the quality of the numerical simulation, we compute the Wronskian $W = \phi_1\,(y)\,\phi_2'\,(y) - \phi_2\,(y)\,\phi_1'\,(y)$. From the general theory of differential equations of second order, we know that W does not depend on y. Here, from the values of ϕ_1 and ϕ_2 at $y = 0$, given by their definition, we have $W = 1$. We test the accuracy of this in all our numerical simulations. For instance in the case of simple critical layers, using the matlab function *ode45,* and fixing the relative error and the absolute error parameters of this function to 10^{-13}, we obtain solutions for which errors in W are typically smaller than 10^{-6} for $\epsilon = 10^{-4}$.

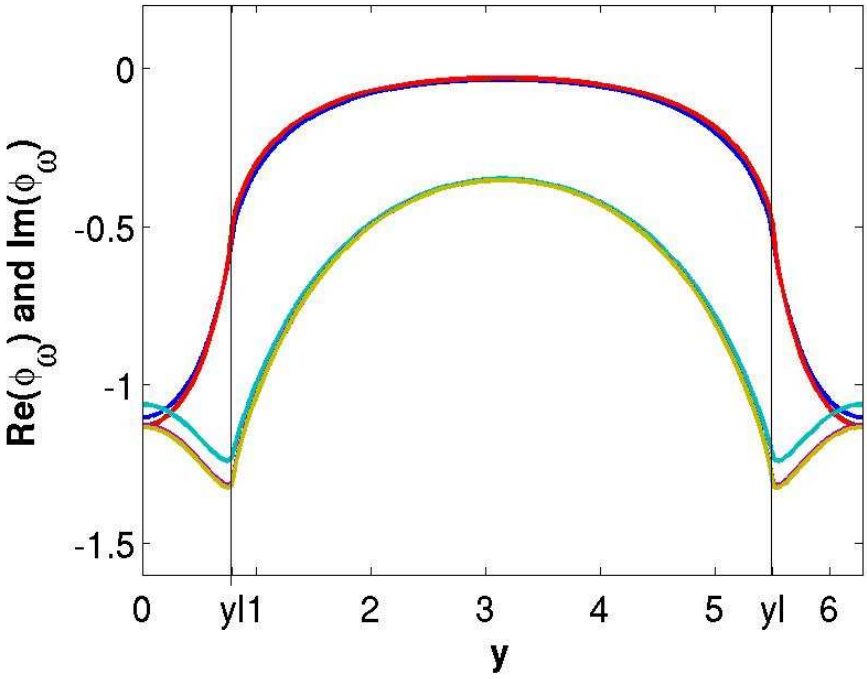

Figure 2: The real and the imaginary part for the solution $\phi_\omega\left(y, c+i\epsilon\right)$ to the inhomogeneous Rayleigh equation (9), in the case $\omega(y,0)=1$, $c=\sqrt{2}/2$ ($y_l=\pi/4$ and $y_l=7\pi/4$), $k=1.5$. The different curves show the results for $\epsilon=10^{-2}$, $\epsilon=10^{-3}$ and $\epsilon=10^{-4}$. The curves for $\epsilon=10^{-3}$ and $\epsilon=10^{-4}$ are indistinguishable, showing good convergence. The imaginary part is the ensemble of curves with a kink close to the critical layers.

Figure 2 shows the real and the imaginary part for the solution $\phi_\omega\left(y, c+i\epsilon\right)$ to the inhomogeneous Rayleigh equation (9), in the case $\omega(y,0)=1$, $c=\sqrt{2}/2$ ($y_l=\pi/4$ and $y_l=7\pi/4$), $k=1.5$ for the values $\epsilon=10^{-2}$, $\epsilon=10^{-3}$ and $\epsilon=10^{-4}$. This illustrate the convergence of the solutions $\phi_\omega\left(y, c+i\epsilon\right)$ to a continuous function $\phi_\omega\left(y, c+i0\right)$. The visible kinks close to the critical layers suggest the discontinuity of the derivative. This is actually verified and illustrated in figure 3, that shows the derivative with respect to y, $\phi'_\omega\left(y, c+i\epsilon\right)$.

2.3.3 Limit $\epsilon \to 0^+$ for critical layer of stationary streamlines

We now consider the case of a critical layer that correspond to a stationary streamline ($y_l=y_0$, where $U(y_0)=c_0$, $U'(y_0)=0$ and $U''\left(y_0\right)\neq 0$).

In order to properly study the limit $\epsilon\to 0$ in this case, we first build a solution to the homogeneous equation (10), which is regular at the critical layer $y=y_0$. We define $\phi_r\left(y, c_0\right)$ as the solution to (10) with $\phi_r\left(y_0, c_0\right)=0$, $\phi_r^{'}\left(y_0, c_0\right)=0$ and $\phi_r^{''}\left(y_0, c_0\right)=1$. Such a solution can be shown to exist by a series expansion in powers of $(y-y_0)$. It can be shown that $\phi_r\left(y, c_0\right)$ is an analytic function of y in the vicinity of y_0, if we suppose that $U\left(y\right)$ is analytic in the vicinity of y_0.

However, by contrast to the case of isolated critical layers analyzed in section (2.3.2), the solution $\phi_r\left(y, c_0\right)$ is not analytic in the vicinity of c_0.

Let us first prove that it exists a solution to the inhomogeneous Rayleigh equation, for $\epsilon=0$, which is continuously differentiable at y_0. We start from expression (18). f is analytic in y_0. Let us choose $e=-f(y_0)$ and $b=0$. Then we obtain the particular solution

$$\phi_{\omega,0}(y)=\phi_r(y)\int_{y_0}^{y}\frac{\left(f-f\left(y_0\right)\right)}{\phi_r^2}. \tag{25}$$

Noting that the expansion of ϕ_r begins at order 2 in $(y-y_0)$, we easily prove that

$$\phi_{\omega,0}(y)=\phi_i\left(y\right)+g\phi_r\left(y\right)\log\left|y-y_0\right|, \tag{26}$$

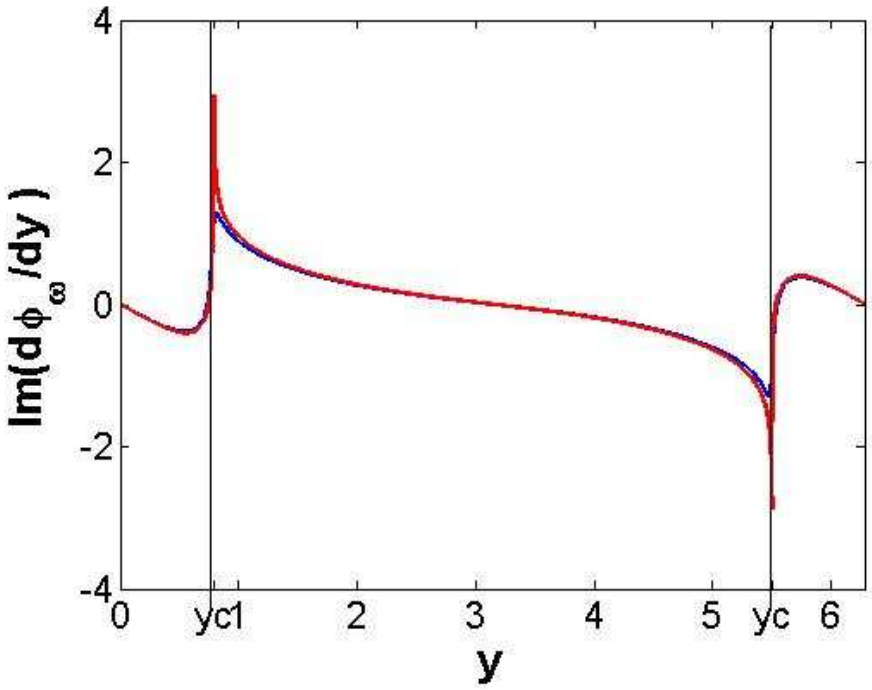

Figure 3: Same as the previous figure, but for the imaginary part of the derivative $\phi'_\omega(y, c + i\epsilon)$ of the solution to the inhomogeneous Rayleigh equation (9).

where g is a constant and ϕ_i is an analytic function of y. We note that $\phi_{\omega,0}(y)$ is continuously differentiable at the critical layer y_0. This solution is defined locally, in an interval where ϕ_r has no other zero than y_0. However, it can be extended to the whole interval $y \in (0, 2\pi)$, because equation (9) is not singular in other points than y_0.

By contrast to the situation obtained for isolated critical points, we can not make an analytical continuation of the solution (25) for complex $c_0 + i\epsilon$. We thus follow another route.

We note that we can add $b\phi_i$ to $\phi_{\omega,0}(y)$, where two different values for b can be chosen for $y < y_0$ and for $y > y_0$. The function

$$\begin{cases} \phi_+(y, c_0) = b^- \phi_r(y) + \phi_{\omega,0}(y) \text{ for } y < y_0 \\ \phi_+(y, c_0) = b^+ \phi_r(y) + \phi_{\omega,0}(y) \text{ for } y > y_0 \end{cases} \tag{27}$$

is actually a solution to the inhomogeneous Rayleigh equation (9) for any $y \neq y_0$ which is continuously differentiable in y_l. It is thus a solution to (9).

The values of b^+ and b^- can be chosen in order to satisfy the boundary conditions. For instance, for 2π-periodic solutions, we obtain

$$N \begin{pmatrix} b^- \\ b^+ \end{pmatrix} = \begin{pmatrix} \phi_{\omega,0}(2\pi) - \phi_{\omega,0}(0) \\ \phi'_{\omega,0}(2\pi) - \phi'_{\omega,0}(0) \end{pmatrix} \text{ with } N = \begin{pmatrix} \phi_r(0) & -\phi_r(2\pi) \\ \phi'_r(0) & -\phi'_r(2\pi) \end{pmatrix} \tag{28}$$

The determinant of N then plays the role of a dispersion relation for neutral mode associated to the stationary streamlines. It reads

$$D_s = -\phi_r(0)\phi'_r(2\pi) + \phi_r(2\pi)\phi'_r(0) \tag{29}$$

When no such mode exists, equation (28) is solved, and we obtain a solution to the inhomogeneous Rayleigh equation that verifies the boundary conditions.

We have thus constructed a solution to the inhomogeneous Rayleigh equation for real $c_0 = U(y_0)$, where y_0 is a stationary point of U such that $U''(y_0) \neq 0$.

We illustrate the preceding results with numerical solutions of the inhomogeneous Rayleigh equations on a doubly periodic domain, for the Kolmogorov base flow $U(y) = \cos y$.

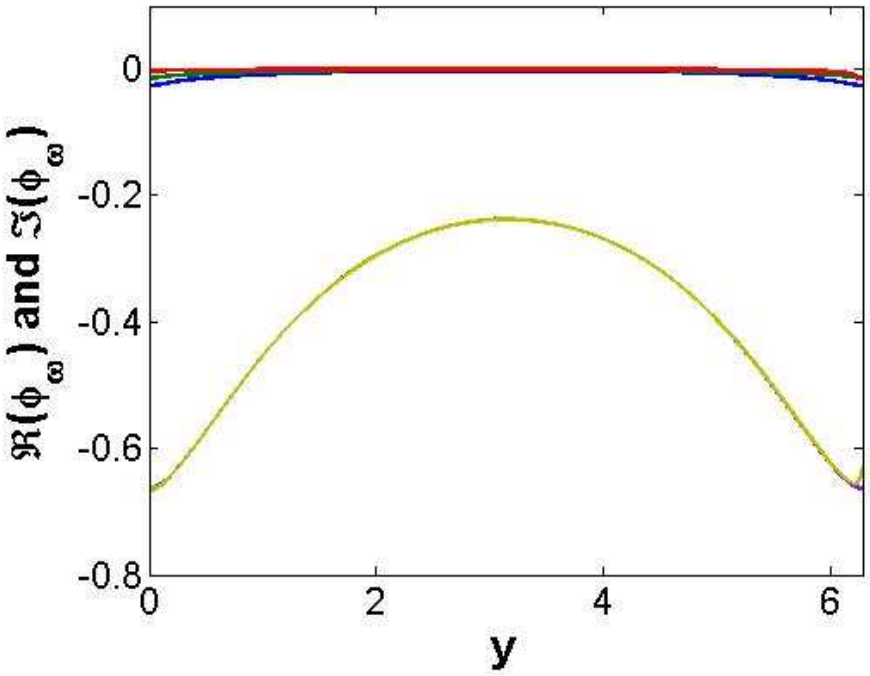

Figure 4: The real and the imaginary part for the solution $\phi_\omega(y, c_0 + i\epsilon)$ to the inhomogeneous Rayleigh equation (9), in the case $\omega(y,0) = 1$; with a critical layer corresponding to a stationary point ($c_0 = 1$, $y_l = 0$) and with $k = 1.5$. The different curves show the results for $\epsilon = 10^{-2}$, $\epsilon = 5.10^{-3}$ and $\epsilon = 10^{-3}$. The curves for $\epsilon = 5.10^{-3}$ and $\epsilon = 10^{-3}$ are indistinguishable, showing good convergence. The real part is the ensemble of curves that converge to zero.

The numerical computation follows the same rules are the one described in section 2.3.2. We note that using the matlab function *ode45,* and fixing the relative error and the absolute error parameters of this function to 10^{-13}, we obtain solutions for which errors in W are typically smaller than 10^{-2} for $\epsilon = 10^{-3}$. It is thus much harder to obtain good quality numerical simulation in that case, than in the case of isolated critical layers discussed in section 2.3.2.

Figure 4 shows the real and the imaginary part for the solution $\phi_\omega(y, c_0 + i\epsilon)$ to the inhomogeneous Rayleigh equation (9), in the case $\omega(y,0) = 1$; with a critical layer corresponding to a stationary point ($c_0 = 1$, $y_0 = 0$) and with $k = 1.5$; for the values $\epsilon = 10^{-2}$, $\epsilon = 5.10^{-3}$ and $\epsilon = 10^{-3}$. This illustrates the convergence of the solutions $\phi_\omega(y, c_0 + i\epsilon)$ to a continuous function $\phi_+(y, c_0)$. It turns out that the real part converges to zero. The same results are also presented for the derivative with respect to y, $\phi'_\omega(y, c_0 + i\epsilon)$, on figure 5.

We now turn to the derivation of a property of such solutions, that will be very important in the discussion of the asymptotic behavior of the linearized Euler equation. We have shown that $\phi_+(y, c_0)$ is continuously differentiable at y_l, and has a second order logarithmic singularity at y_0 (see (26) and (27)). Then a direct inspection of the leading singularity in equation (9), of order $(y - y_c)^{-1}$, leads to the conclusion that

$$ikU''(y_0)\,\phi_+(y_0, U(y_0)) + \omega(y_0, 0) = 0 \tag{30}$$

2.3.4 The asymptotic vorticity field

Using the results of the previous section, we prove in this section that the vorticity field converges, for large time, towards a field oscillating at a multiple of the streamline frequency. More precisely, we prove that

$$\omega(y,t) \underset{t\to\infty}{\sim} \omega_\infty(y) \exp(-ikU(y)t) + \mathcal{O}\left(\frac{1}{t^\gamma}\right) \tag{31}$$

In particular, for any stationary point y_0, $\omega_\infty(y_0) = 0$. This essential property means that the vorticity cancels rapidly at any stationary streamline. This is the mechanism of vorticity depletion at the stationary streamlines,

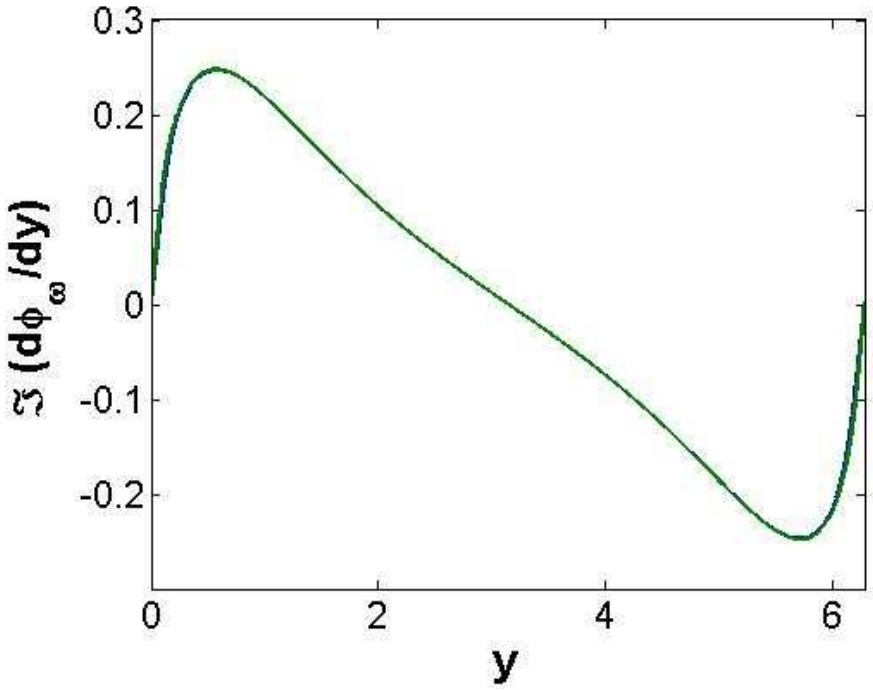

Figure 5: Same as the previous figure, but for the imaginary part of the derivative $\phi'_\omega(y, c_0 + i\epsilon)$ of the solution to the inhomogeneous Rayleigh equation (9).

discussed in the introduction.

Using (11) and (8) we have

$$\hat{\omega}(y, c + i\epsilon) \underset{\epsilon \to 0^+}{\sim} \frac{ikU''(y)\,\phi_+(y,c) + \omega(y,0)}{ik\,(U(y) - c - i0^+)} \tag{32}$$

We thus see that for any c, $\hat{\omega}(.,c)$ has singularities for any critical layer y_l. For fixed y, $\hat{\omega}(y,.)$ has a single singularity for the velocity $c = U(y)$. Using (32), we write the inverse Laplace transform (7) on the Bromwich contour defined by $p = -ik(c + i\epsilon)$ with $\epsilon > 0$ and $-\infty \leq c \leq +\infty$.

$$\omega(y,t) = \frac{1}{2\pi i} \int_{-\infty}^{+\infty} dc\, \frac{\exp(-ik(c+i\epsilon)t)}{U(y) - c - i\epsilon} [ikU''(y)\,\phi(y, c + i\epsilon) + \omega(0,y)] \tag{33}$$

We first estimate the contribution of the pole

$$\frac{1}{2\pi i} \int_{-\infty}^{+\infty} dc\, \frac{\exp(-ik(c+i\epsilon)t)}{U(y) - c - i\epsilon} [ikU''(y)\,\phi_+(y,U(y)) + \omega(0,y)] = [ikU''(y)\,\phi_+(y,U(y)) + \omega(y,0)] \exp(-ikU(y)t),$$

using the standard deformation of the contour of the complex integral, and the residue theorem. The remainder contribution to the vorticity (33) is then

$$\frac{kU''(y)}{2\pi} \int_{-\infty}^{+\infty} dc\, \frac{\phi_+(y,c) - \phi_+(y,U(y))}{U(y) - c} \exp(-ikct).$$

This integral is an oscillating integral. For large times, it thus gives a contribution of order $\mathcal{O}(1/t^\gamma)$ where γ depends on the order differentiability of $\phi_+(y,c)$ as a function of c. The result (31) is thus proved, and we have

$$\omega_\infty(y) = ikU''(y)\,\phi_+(y,U(y)) + \omega(y,0). \tag{34}$$

We remark that for any point in the flow y_1 where $U''(y_1)$ vanishes, $\omega_\infty(y_1) = \omega(y_1, 0)$. This could have been anticipated as for such points y_1, from (6), we trivially have $\omega(y_1,t) = \omega(y_1,0)\exp(-ikU(y_1)\,t)$ for any

time t.

Using (30) and (34), we deduce that

$$\omega_\infty(y_0) = 0,$$

This result means that the vorticity tends to zero for large time for any stationary streamlines y_0. This vorticity depletion at the stationary streamline is, from a mathematical point of view, a nontrivial consequence of the Laplace transform analysis, and of the regularization of the resolvent operator at stationary velocities. As will be illustrated in section 4, using numerical simulation, it is a striking dynamical effect leading to the disappearance of any filament in the area close to the critical layer of a stationary point of the profile U. This has a large qualitative impact on the flow structure and evolution.

This effect comes from the term $v_y U''(y)$ in the linearized Euler equation (6) ; it is thus a consequence of the effect of the transverse velocity on the background vorticity. Because v_y is a non local quantity, depending on the evolution of the vorticity field everywhere in the domain, this effect is a non local trivial one that we are not able to explain easily heuristically.

Besides these theoretical results, the Laplace tools are very interesting as they allow the computation of asymptotic behavior of the flow without relying on a complex direct numerical computation. Moreover, whereas in asymptotic approaches like the Lundgren's one, the asymptotic profile $\omega_\infty(y)$ is not determined, here we can compute it from (34).

Using this last procedure and the numerical computations of the resolvent ϕ_ω, described in sections 2.3.2 and 2.3.3, we compute asymptotic vorticity profiles. They are represented in Figure 9 and Figure 10 and discussed in more details in section 4.3.

2.3.5 The asymptotic velocity field

In this section we study the asymptotic behavior of the velocity field. We prove that the velocity field decays algebraically for large times :

$$v_x(y,t) \underset{t\to\infty}{\sim} \frac{\omega_\infty(y)}{ikU'(y)} \frac{\exp(-ikU(y)t)}{t} \text{ and} \tag{35}$$

$$v_y(y,t) \underset{t\to\infty}{\sim} \frac{\omega_\infty(y)}{ik\left(U'(y)\right)^2} \frac{\exp(-ikU(y)t)}{t^2}; \tag{36}$$

where ω_∞ is the asymptotic vorticity profile (31,34).

We first explain this result starting from the asymptotic vorticity derived in the previous section (31), and using large time asymptotic behavior of oscillating integrals. This argument is heuristically very interesting. However it will be valid only when the contributions of stationary points y_0 are negligible, and when the convergence of the vorticity towards the asymptotic vorticity is sufficiently rapid. Indeed, the convergence towards the Lundgren's ansatz has to be uniformly more rapid than the derived algebraic laws. This last point is actually true only for strictly monotonic velocity profiles U as will be discussed below.

In order to give a proof of the results (35) and (35) valid for also for profile U with stationary streamlines, we give a more general argument based on Laplace transform at the end of this section.

Oscillating integrals We begin with the expression of the velocity from the vorticity field using a Green function formalism. We have

$$\mathbf{v}(y,t) = \int dy'\, \mathbf{G}_k(y,y')\omega(y',t). \tag{37}$$

$\mathbf{G}_k$ is defined from (5) :

$$\mathbf{G}_k(y,y') = \left(-\frac{\partial H_k}{\partial y}, ikH_k\right)(y,y') \text{ with } \frac{\partial^2 H_k}{\partial y^2} - k^2 H_k = \delta(y-y'),$$

with the periodic boundary conditions on y. Using the asymptotic result on the vorticity field, we thus have

$$\mathbf{v}(y,t) \underset{t\to\infty}{\sim} \int dy'\, \mathbf{G}_k(y,y')\,\omega_\infty(y')\exp(-ikU(y)t). \tag{38}$$

We consider the asymptotic behavior, for large times t, of the oscillating integral (38). Since Kelvin, very classical results do exist for the asymptotic behavior of such integrals, the most well known results being the stationary phase approximation. Such results are discussed in appendix A.

An essential point, which differentiate our approach from the classical framework, is that the Green function $\mathbf{G}_k(y,y')$ is not smooth everywhere : it is smooth except for the singularity when $y=y'$. We prove in appendix A that *if $U(y)$ has no stationary points* (for all y, $U'(y)\neq 0$)**,** then results (35-36) are valid, the main contribution being related to the singularities of the Green function.

If the velocity field $U(y)$ has M stationary points y_m ($U'(y_m)=0$), then the contributions of the stationary points, generically of order $1/\sqrt{t}$, usually dominate the contributions of the singularity of the Green function $\mathbf{G}_k$, in integrals like (38). If $\omega_\infty(y_m)\neq 0$, the classical stationary phase approximation (see appendix A) would lead to

$$\mathbf{v}(y,t) \underset{t\to\infty}{\sim} \sum_{m=1..M} \mathbf{G}_k(y,y_m)\omega_\infty(y_m)\sqrt{\frac{2\pi}{|kU''(y_m)|}}\exp\left(\frac{i\epsilon_m\pi}{4}\right)\frac{\exp(-ikU(y_m)t)}{\sqrt{t}},$$

where ϵ_m is the sign of $-kU''(y_m)$.

However, a remarkable fact is that for any stationary point y_0 (such that $U'(y_0)=0$), due to the vorticity depletion mechanism discussed in section 2.3.4 and proved in section 2.3.3, $\omega_\infty(y_0)=0$. Then the leading order contribution from the stationary phase approximation vanishes. The analysis could proceed in order to determine the next leading order term in the expansion, from (38), expected to be of order $1/t^{3/2}$. However, such a detailed analysis is useless, because the convergence of $\omega(.,t)$ towards the asymptotic vorticity profile ω_∞ is too slow, in the vicinity of a stationary streamline. Actually the error due to the slow convergence towards the Lundren's profile gives contributions which are also of order $1/t^{3/2}$. This will be illustrated using direct numerical simulations in section 4 (see figure 8 page 21, figure 14 page 26 and the related text).

Laplace tools In order to give a precise argument for the results (35-36), we use Laplace tools. We first note that $v_y=ik\psi$, and study the asymptotics for the stream function ψ. Starting from inverse Laplace transform of ψ, we have

$$\psi(y,t)=\frac{k}{2\pi}\int_\infty^{+\infty} dc\,\phi_+(y,c)\exp(-ikct), \tag{39}$$

where $\phi_+(y,.)$ is the limit of $\phi(y,c+i\epsilon)$ for $\epsilon\to 0$. (39) is an oscillating integral. We use that for any y for which $U'(y)\neq 0$, $\phi_+(y,c)$ is twice differentiable except at $c=U(y)$ where it has a logarithmic singularity $\Delta\phi_c(c-U(y))\log(c-U(y))$ (see equation (23)). Then the large time asymptotics of ψ is due to this singularity. In order to evaluate it, we part integrate twice (39) and evaluate the contribution of the singularity with the residue theorem. Then the leading order contribution is obtained as,

$$\psi(y,t) \underset{t\to\infty}{\sim} \frac{\omega_\infty(y)}{(ikU'(y))^2}\frac{\exp(-ikU(y)t)}{t^2}, \tag{40}$$

where we have used (24) and (34) in order to express $\Delta\phi_c$.

We note that (36) follows immediately from (40) and $v_y=ik\psi$. The asymptotic result (35) for the transverse velocity v_x can be derived by following similar arguments as the one just described for ψ.

The above argument uses the explicit prediction (23) for the singularity of $\phi_+(y,c)$ as a function of c. The expressions (23) and (24) are valid only when y is not a stationary streamline ($U'(y)\neq 0$). For stationary streamlines y_m we have no theoretical predictions. Direct numerical computation in section 4.3 will lead us to conjecture that for such special points $\psi(y_m,t) \underset{t\to\infty}{\sim} C_1\exp(-ikU(y_m)t)/t^{3/2}$, $v_x(y_m,t) \underset{t\to\infty}{\sim} C_2\exp(-ikU(y_m)t)/t^{3/2}$ and $v_y(y_m,t) \underset{t\to\infty}{\sim} ikC_1\exp(-ikU(y_m)t)/t^{3/2}$. We not that this exponent $3/2$ is not related to a contribution from the stationary phase approximation.

We thus conclude that the results (35) and (36) are valid for monotonic profiles, but also for base flow with stationary streamlines. This is in marked contrast to what was thought in many previous publications based on the asymptotic expansions and the stationary phase arguments. This is mainly due to the vorticity depletion mechanism at the stationary streamlines discussed in the previous section. We also stress that, using Laplace tools, the asymptotic profile $v_\infty(y)$ can be numerically computed easily, without relying on direct numerical computations of the Euler equations.

We have no theoretical prediction for the power law in the asymptotic behavior of the perturbation velocity, in the special case of stationary streamlines.

3 Asymptotic stability of the Euler equation

In the previous section, we have obtained results for the asymptotic behavior of the linearized Euler equations, with initial conditions close to some parallel flows $\mathbf{v}_0(\mathbf{r}) = U(y)\,\mathbf{e}_x$. We now address the evolution of the same initial conditions by the nonlinear Euler equation (3). The aim of this section is to explain why the linearized dynamics will be a good approximation for the dynamics for any time t, and to explain why the flow velocity is asymptotically stable (in kinetic energy norm).

We consider the initial vorticity $\Omega(x,y,0) = -U'(y) + \epsilon\omega(x,y,0)$, where ϵ is small. We suppose, without loss of generality that $\int dx\,\omega = 0$. The perturbation ω can be decomposed in Fourier modes along the x direction

$$\omega(x,y,t) = \sum_k \omega_k(y,t)\exp(ikx).$$

From the Euler equations (3), the equation for the evolution of ω_k reads

$$\frac{\partial\omega_k}{\partial t} + ikU(y)\,\omega_k - ik\psi_k U''(y) = -\epsilon NL \text{ with } NL = \sum_l \left\{ -ik\frac{\partial\psi_l}{\partial y}(y,t)\,\omega_{k-l}(y,t) + \frac{\partial}{\partial y}\left[il\psi_l(y,t)\,\omega_{k-l}(y,t)\right]\right\}. \tag{41}$$

The left hand side is the linearized Euler equation, whereas the right hand side are the nonlinear corrections. We want to prove that, for sufficiently small ϵ, neglecting the nonlinear terms is self-consistent.

For this we have to prove that the nonlinear terms remains uniformly negligible for large time. We then use the asymptotic results for the linearized equation derived in section (2). We thus have, for any k

$$\psi_{k,L}(y,t) \underset{t\to\infty}{\sim} \frac{\omega_{k,L,\infty}(y)}{(ikU'(y))^2}\frac{\exp(-ikU(y)t)}{t^2} \text{ and } \omega_{k,L}(y,t) \underset{t\to\infty}{\sim} \omega_{k,L,\infty}(y)\exp(-ikU(y)t), \tag{42}$$

where the subscript L refers to the evolution according to the linearized dynamics. We call a quasilinear approximation to the right hand side of equation (41), the approximation where ψ_k and ω_k would be evaluated according to their linearized evolution close to the base flow $U(y)$. From (42), one would expect at first sight that this quasilinear approximation of the nonlinear term NL_{QL}, would give contributions of order $O(1/t)$. The detailed computation, easily performed from (42), actually shows that the contributions of order $O(1/t)$ identically vanish for large times. Then

$$\epsilon NL_{k,QL} \underset{t\to\infty}{=} O\left(\frac{\epsilon}{t^2}\right)$$

This is an important remark, as it proves that within a quasilinear approximation, the contribution of the nonlinear terms NL_{QL} remains uniformly bounded, and more importantly it is integrable with respect to time.

Then it is natural to conjecture that the contribution of the nonlinear terms remains always negligible. More precisely, we naturally conjecture, that within the fully nonlinear equation, for sufficiently small ϵ:

$$\psi_k(y,t) \underset{t\to\infty}{\sim} \frac{\omega_{k,\infty}(y)}{(ikU'(y))^2}\frac{\exp(-ikU(y)t)}{t^2} \text{ and } \omega_k(y,t) \underset{t\to\infty}{\sim} \omega_{k,\infty}(y)\exp(-ikU(y)t)$$

with

$$\omega_{k,\infty}(y) = \omega_{k,L,\infty}(y) + O(\epsilon)$$

A similar reasoning in order to evaluate the nonlinear evolution for the profile $U(y)$ would lead to the conclusion that for large times

$$\Omega_0(y,t) \underset{t\to\infty}{\sim} -U'_\infty(y) \text{ with } U'_\infty(y) = U(y) + \delta U(y)$$

where $\delta U = O(\epsilon^2)$.

This means that the parallel flow will quickly stabilize again towards another parallel flow which is close to the initial one.

A natural question would be to compute the modified profile. The preceding analysis leads to the quasilinear expression

$$\delta U(y) = -\epsilon^2 \int_0^\infty dt\, NL_{0,QL}(t) + o(\epsilon^2) \tag{43}$$

This expression involves integrals over times of the linearized Euler equation. It is not amenable to simple expression.

This result has to be contrasted with the results usually obtained using a Quasi-Linear approach. Usually the integral occurring in (43) diverges. Then one invokes a time scale separation, and the divergence of the integral is regularized using a multiple scale analysis. Here, by contrast, the integral converges. This means that there is a single time scale over which all quantities reach their asymptotic value (a typical time scale here is $1/s$ where s is the typical shear). The nonlinear evolution is thus very brief and leads to very small changes in the initial profile U. Then any references to Markovian approximations would be both misleading and useless.

From this discussion, we thus conclude that any profile U verifying the hypothesis of this work (no unstable and no neutral modes for the linearized dynamics) is asymptotically stable. We have not given a mathematical proof of this, but we have explained that a quasilinear description of this nonlinear evolution is self-consistent and leads to this conclusion.

4 The Kolmogorov flow

In this section, we consider the particular case of the 2D Euler equations in a doubly periodic domain $\mathcal{D} = [0, 2\pi/\delta)\,[0, 2\pi)$, where $\delta > 1$ is the aspect ratio ; with the Kolmogorov base flow $U(y) = \cos(y)$.

4.1 Stability

4.1.1 Lyapounov stability

We consider initial vorticity conditions close to the base flow vorticity $\omega_0(y) = \sin(y)$. We let this initial condition evolve according to the nonlinear Euler equation (3). If the perturbation to the initial flow remains small for all times, the flow is said to be Lyapounov stable. We first prove that the base flow $\omega_0(y)$ is Lyapounov stable as soon as $\delta > 1$.

The classical Energy-Casimir method proposed by Arnold [2] cannot be applied directly here. Indeed, the Kolmogorov flow does not verify the hypothesis for any of the two Arnold theorems [2]. However, we can still prove the stability in this case, by direct analysis. Let us define the energy-Casimir functional F as

$$F[\Omega] = \frac{1}{2}\int_{\mathcal{D}} \left(\Omega^2 - \mathbf{V}^2\right)$$

F is the enstrophy minus the kinetic energy of the flow. It is thus a conserved quantity for the Euler equations.

We use the fact that the base flow $\omega_0(y) = \sin(y)$ ($\mathbf{v}_0 = \cos(y)\,\mathbf{e}_x$) is a minima of F. We first consider the perturbation vorticity $\omega = \Omega - \omega_0$, and we decompose it into Fourier modes $\omega = \sum_{k>1} \omega_k e_k$ with $\Delta e_k = -\lambda_k e_k$ where the $\lambda_k > 0$ are arranged in increasing order, and where e_k are orthonormal ($\int_{\mathcal{D}} e_k e_{k'} = \delta_{kk'}$). On a doubly periodic domain $\mathcal{D} = [0, 2\pi/\delta)\,[0, 2\pi)$, if $\delta > 1$, we have $\lambda_1 = \lambda_2 = 1$ corresponding for instance to the $\cos(y)$ and $\sin(y)$ modes. Then for any $k \geq 3$, $\lambda_k > 1$.

We obtain

$$F = \frac{1}{2}\sum_k \frac{\lambda_k - 1}{\lambda_k}\omega_k^2 \tag{44}$$

Thus, because $\lambda_k \geq 1$, $F \geq 0$. Moreover $F[\omega_0] = 0$. We thus conclude that ω_0 is a global minimum for F.

We note that this minimum is degenerate, because all vorticity fields $\omega = \alpha\cos(y) + \beta\sin(y)$ are also minima.

Because F is a conserved quantity, we conclude that

$$\frac{1}{2}\sum_{k\geq 3} \frac{\lambda_k - 1}{\lambda_k}\omega_k^2(t) = \varepsilon_F, \tag{45}$$

where $\varepsilon_F = F(0)$ is the small value of F for the initial perturbation. Then if they are initially small, all ω_k for $k \geq 3$ remain small for large times, the amplitude being measured according to the norm (44).

Expression (45) does not control the first Fourier modes Ω_1 and Ω_2. For this, we use the fact that the enstrophy

$$\Gamma_2 = \frac{1}{2}\int_{\mathcal{D}} \Omega^2$$

is conserved. We suppose that its initial value is $\Gamma_{2,0} + \epsilon_\Gamma$ where $\Gamma_{2,0}$ is the base flow enstrophy and ϵ_Γ is the perturbation enstrophy. Using the enstrophy conservation we have

$$\Omega_1^2(t) + \Omega_2^2(t) = 2\Gamma_{2,0} + 2\epsilon_\Gamma - \sum_k \omega_k^2.$$

Then, using that $\sum_{k\geq 3} \omega_k^2 \leq \frac{2\lambda_3}{\lambda_3 - 1}\epsilon_F$ (derived from (45), using $\lambda_k \geq \lambda_3$ for $k \geq 3$), we have

$$\left|\Omega_1^2(t) + \Omega_2^2(t) - 2\Gamma_{2,0}\right| \leq 2\max\left\{\epsilon_\Gamma, \frac{\lambda_3}{\lambda_3 - 1}\epsilon_F\right\}.$$

This means that the flow associated to the two first mode is $a(t)\sin(y + \phi(t))$ where ϕ may be arbitrary but where the amplitude a is controlled up to an error of order $\max\{\epsilon_\Gamma, \epsilon_F\}$.

We have thus proved that any initial condition close to the initial profile $\omega = \sin(y)$ remains close to the family of profiles $\sin(y + \phi)$. Then the flow is Lyapounov stable in this restricted meaning.

4.1.2 Linear and spectral stability

Next, we let the initial conditions close to the base flow $\omega_0(y) = \sin y$ evolve according to the linearized Euler equation (4). If the perturbation to the initial flow remains small for this dynamics, the flow is said to be linearly stable.

We decompose the perturbation vorticity in a Fourier series for the x variable only. For parallel flows, due the translational invariance, such Fourier modes are independent. The modes with no dependence on x are easily shown to be neutral. Then the only issue is about the stability of other modes. In order to prove this, we simply note that the perturbed Energy-Casimir functional (44) is conserved not only by the nonlinear Euler dynamics but also by the linearized one. Then, because the Energy-Casimir functional is positive, this proves that any x-dependent perturbation remains small if it is initially small. The flow is thus linearly stable as soon as $\delta > 1$.

If the linear equation has no exponentially growing modes, it is called spectrally stable. Linear stability implies spectral stability (the converse may be wrong). Then because it is linearly stable, we can conclude that no unstable modes exist to the linearized Euler equation as soon as $\delta > 1$.

4.2 Neutral modes

We look for the modes of equation (4) such that the stream function is of the form $\psi = \phi(y)\exp(ik(x - ct))$. Then ϕ satisfies the classical Rayleigh equation (10).

As discussed in section 4.1.2, no unstable eigenvalue exists for $k^2 > 1$. Thus only for real values of c can the Rayleigh equation have solutions for $k^2 > 1$. In the following, using numerical simulations, we show that no neutral modes exist, except for the marginal case $k = 1$.

When c is in the range of U : $-1 = \min_y\{U(y)\} < c < 1 = \max_y\{U(y)\}$, $U - c$ vanishes at the two critical layers defined by $U\left(y_{l_{1,2}}\right) = \cos\left(y_{l_{1,2}}\right) = c$. The Rayleigh equation then has logarithmic singularities. As discussed in section 2.1, when initial value problems are considered, the relevant solutions to the Rayleigh equation are the ones that are obtained with $c' = c + i\epsilon$, c real, and by considering the limit $\epsilon \to 0^+$. We study the existence of modes in that limit.

For this, we numerically compute the dispersion relation $D_+(c, k)$ of the Rayleigh equation, as defined in section 2.3.2. Neutral modes correspond to zeros of D_+. We use the same numerical tools as the one described in the end of section 2.3.2 : we use the matlab function *ode45,* and fix a the relative error and the absolute error parameters of this function to 10^{-13}, then obtain solutions for which errors in the Wronskian W are typically smaller than 10^{-6} for $\epsilon = 10^{-4}$. We approximate $D_+(c, k)$ by the numerically computing $D(c + i\epsilon, k)$ with $\epsilon = 10^{-4}$.

Figure 6 shows $D_m(k) = \min_c D^+(c, k)$ (we note that D^+ is unchanged when the sign of k is changed). For a given value of k, some neutral mode exist if and only if $D_m(k)$ vanishes. We conclude from this plot that neutral modes exist only for the value $k^2 = 1$ (we have tested values of k^2 up to $k^2 = 10$).

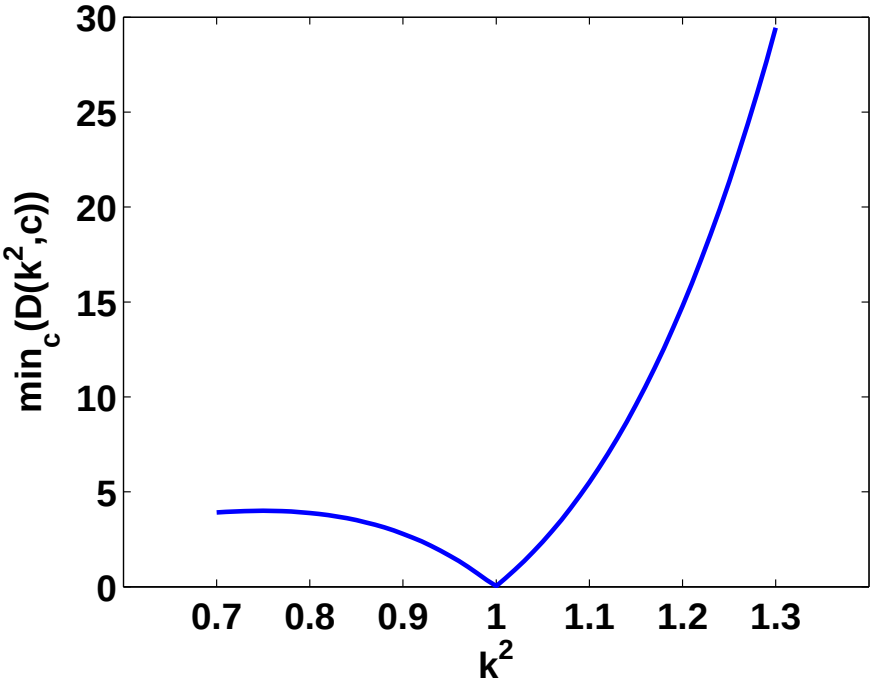

Figure 6: Minimum values for the dispersions relation $\min_c D^+(c,k)$ as a function of k^2. This plot shows that neutral modes exist only for $k^2 = 1$ and are even.

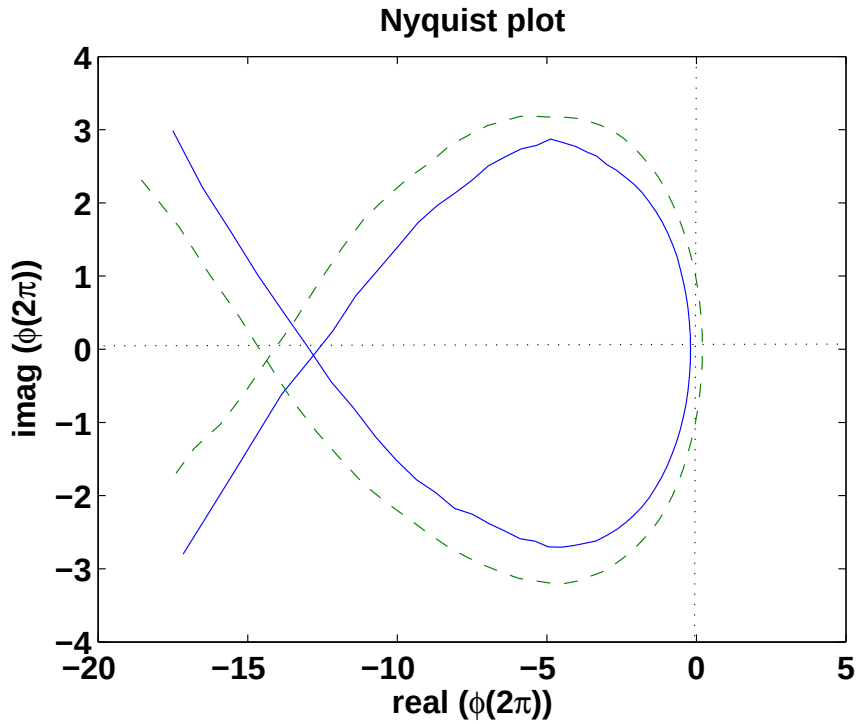

Figure 7: Nyquist plots (complex $D^+(c)$ represented in the complex plane, when c is varied), for values $k^2 = 0.99$ (green dashed line) and $k^2 = 1.01$ (plain blue line).

For $k^2 = 1$, we see numerically that a mode exists for $c = 0$ only. The mode is then trivially found by direct integration of equation (10). It is $\phi = C$ where C is any constant number ($\psi = C\exp(ikx)$ and $\psi = C\exp(-ikx)$).

The representation of the complex curve $D_+(c)$ when c is varied is called a Nyquist plot (see [40] or [5] in the context of fluid dynamics). It is very useful, as the algebraic number of loops of the Nyquist plot around 0 counts the number of unstable modes on the complex half plane $c = c_R + i\lambda$ with positive λ [40, 5].

Figure 7 shows the Nyquist plot of $D_+(c)$, for $k = 0.99$ and $k = 1.01$ respectively. One clearly sees the passing of the curves across the value $D_+ = 0$ when k is changed from $k = 0.99$ to $k = 1.01$, corresponding to neutral modes for $k = 1$. Moreover, we conclude that only one neutral mode exists for this value of k, because only one branch of the curve passes through 0. For larger value of c (not shown), the upper part of the plot loops to the right on the upper half plane goes down to the lower half plane by crossing the real axis for very large values of ϕ, before to close on the branch visible in the lower half plane. Counting the algebraic number of loops around zero, we thus conclude that for $k > 1$, no unstable modes exists, in accordance with the result of section (4.1) ; whereas for $k < 1$ only one unstable mode exists.

From this analysis, we thus conclude that only one neutral mode exists. This modes corresponds to the destabilization of the flow and the appearance of an unstable mode, when passing from values $k^2 \geq 1$ to values $k^2 \leq 1$. It is the trivial mode $\psi = C\exp(ix)$, found for $c = 0$.

4.3 Direct numerical computation of the 2D-Euler equation

In this section, we illustrate and complement the results through the direct numerical simulation of the 2D Euler equations (nonlinear). For the Kolmogorov base flow $U(y) = \cos y$, we apply initial perturbations in the form

$$\omega(x, y, 0) = \epsilon A(y)\cos\delta x \tag{46}$$

with $\epsilon \ll 1$. Since the system is homogeneous in the x direction, it is natural to study the Fourier transform of ω and $\boldsymbol{v}$,

$$\omega_\delta(y,t) = \int \frac{\mathrm{d}x}{2\pi\delta^{-1}}\, \mathrm{e}^{-\mathrm{i}\delta x}\omega(x,y,t) \tag{47}$$

$$\boldsymbol{v}_\delta(y,t) = \int \frac{\mathrm{d}x}{2\pi\delta^{-1}}\, \mathrm{e}^{-\mathrm{i}\delta x}\boldsymbol{v}(x,y,t). \tag{48}$$

First, we consider an initial perturbation where $A(y)$ has the same parity as the base flow velocity one's. In particular, we examine $A(y) = 1$.

Asymptotic vorticity profile for even perturbations. The space-time series of $|\omega_\delta(y,t)|$ is shown in Figure 1, page 4, which we have already seen. Initially, it rapidly (almost exponentially) relaxes toward the final profile, $|\omega_{\delta\infty}(y)|$; in particular, it relaxes to zero at $y = 0$ and π (stationary streamlines), whereas it remains constant at $y = \pi/2$ and $3\pi/2$. The rapid relaxation of the modulus $|\omega_\delta(y,t)|$ is in agreement with the theoretical prediction (31) that the Lundgren ansatz is valid asymptotically.

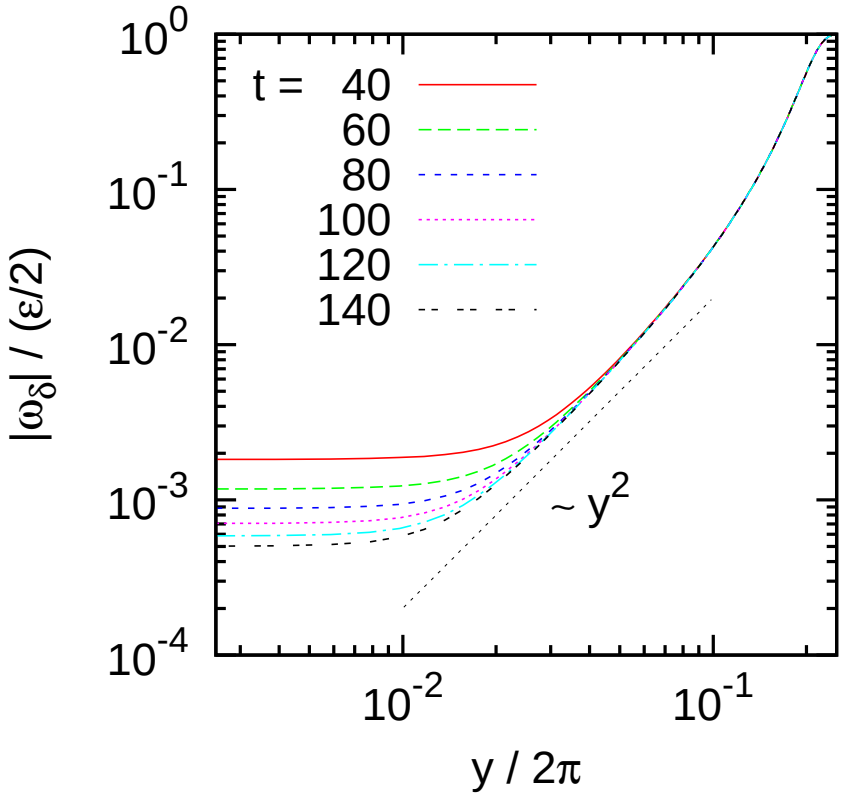

Figure 8: The profiles of perturbation vorticity, $|\omega_\delta(y,t)|$, at several times, for the initial perturbation profile $A(y) = 1$ and aspect ratio $\delta = 1.1$. A flat region is observed near the stationary streamline $y = 0$. As the time goes on, this flat region becomes narrower, and instead, outside of it, a region with a profile proportional to $\sim y^2$ becomes wider, in accordance with a parabolic profile in the large time limit.

After the rapid relaxation, $|\omega_{\delta\infty}(y)|$ converges towards the final profile algebraically. In particular, in the vicinity of $y = 0$ and π (stationary streamlines), it relaxes as slowly as t^{-1}, leading locally to a flat profile (see figure 8). However, as time goes on, this flat region becomes narrower and narrower, and instead away from it a region with a profile proportional to y^2 becomes wider and wider. This indicates that, in the large time limit, the profile is parabolic in the vicinity of the stationary streamlines.

This also illustrates that the relaxation towards the stationary profile does not converge in a uniform way: the process is very slow close to the stationary streamlines whereas it is extremely rapid away from them.

The width y_f of the flat area decreases as $y_f \sim 1/\sqrt{t}$, whereas the constant value of the vorticity modulus in the flat area decreases as $1/t$. When computing the velocity from the vorticity (equation (37)), the overall effect of this flat area is thus of order $1/t^{3/2}$. Such a contribution is thus of the same order as what would give the leading order term of the asymptotic expansion of oscillating integrals, as discussed in the end of section 2.3.5.

In Figure 9, we compare the final profiles obtained from the Laplace tools (equation (34)) and the direct numerical simulations. As shown, the results show a very good agreement. This agreement support both the quality of the direct numerical simulations and the results of the computation of the asymptotic profile from the Laplace transform tools.

The computation of the asymptotic profile from the Laplace methods is extremely rapid and easy, compared with direct numerical simulations. Using this tool, we study some qualitative properties of the asymptotic profile. By increasing the aspect ratio δ, We observe a bifurcation from a single- to a double-peaked asymptotic vorticity profile (Figure 10). The three asymptotic profiles all show the depletion of the vorticity perturbation at the stationary streamlines.

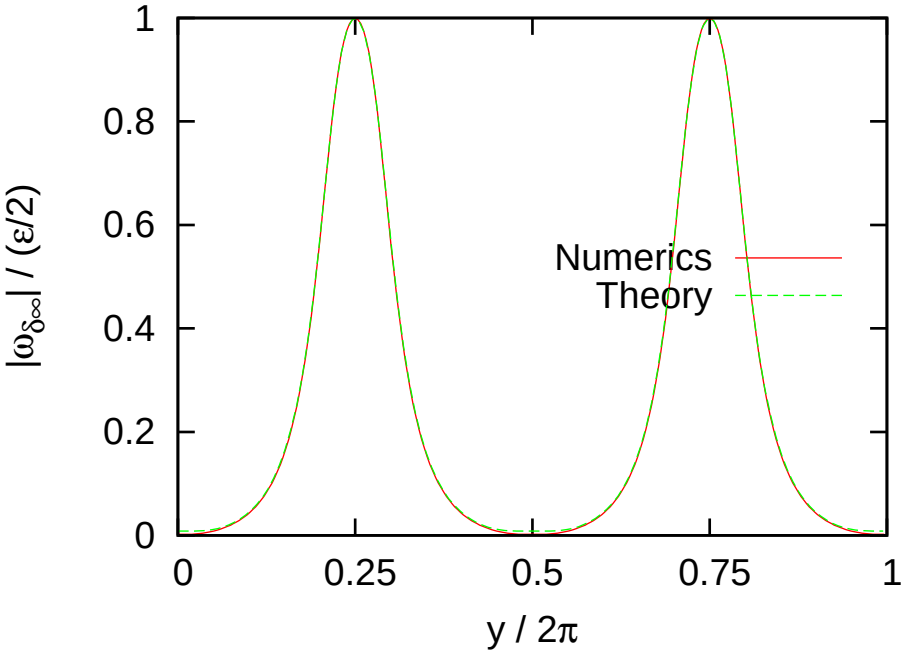

Figure 9: The final profile of the modulus of the perturbation vorticity, $|\omega_{\delta\infty}(y)|$, obtained from the numerics and the theory (equation (34)), for the initial perturbation profile $A(y) = 1$ and the aspect ratio $\delta = 1.1$. The two profiles show a very good agreement.

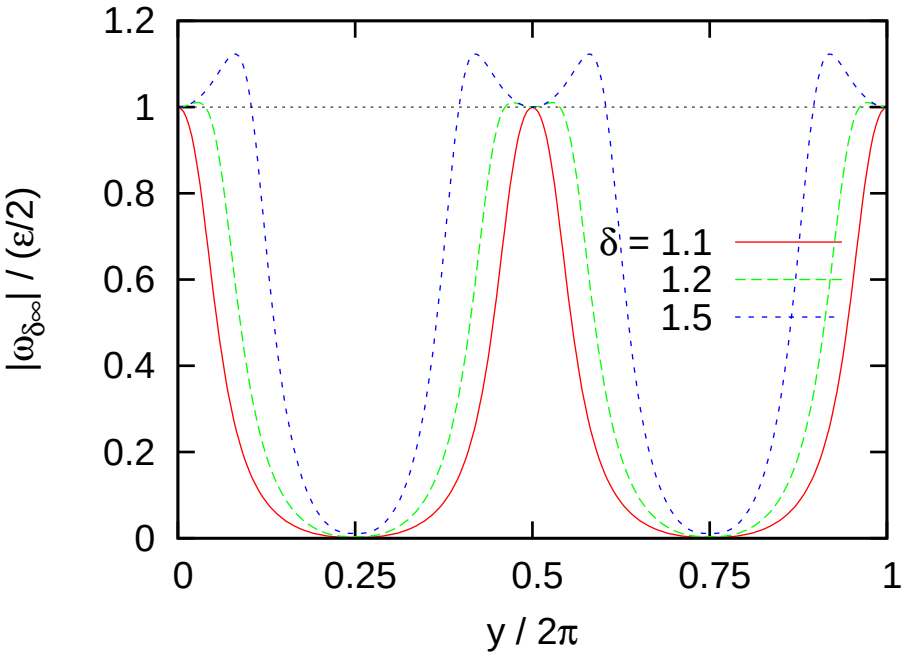

Figure 10: The final profile for the modulus of the perturbation vorticity, $|\omega_{\delta\infty}(y)|$, for the initial perturbation profile $A(y) = 1$, and aspect ratios $\delta = 1.1, 1.2$ and 1.5, computed from the prediction of the Laplace transform tools (equation (34)). The profile shows a bifurcation from single to double peak shapes, when δ is increased.

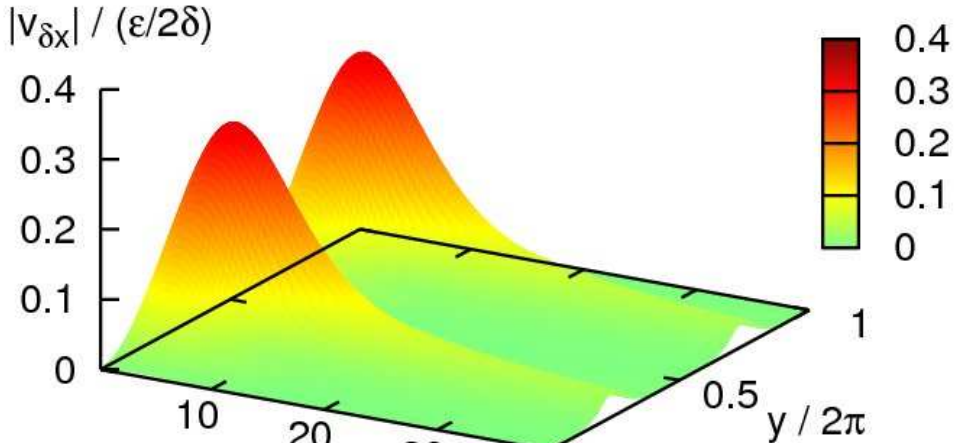

(a)

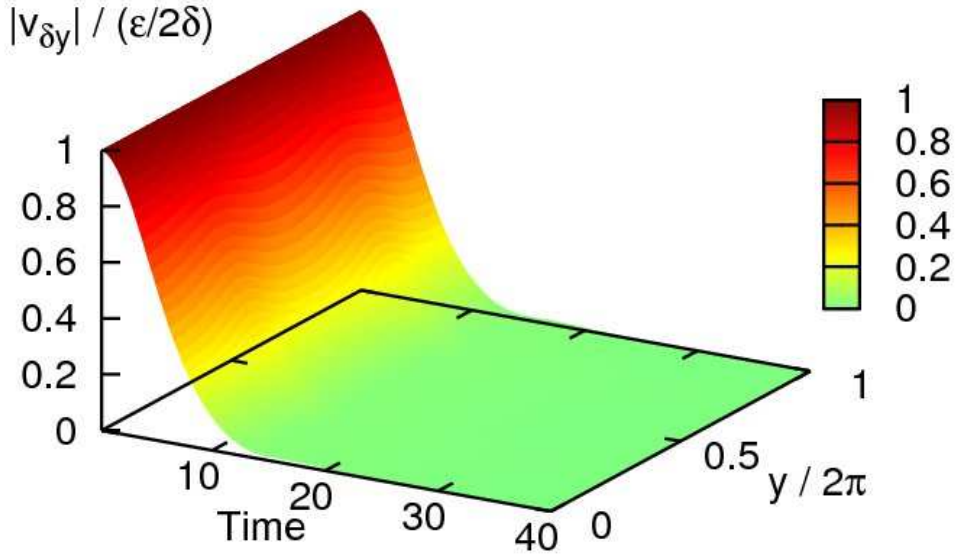

(b)

Figure 11: The space-time series of perturbation velocity components, $|v_{\delta,x}(y,t)|$ (a) and $|v_{\delta,y}(y,t)|$ (b), for the initial perturbation profile $A(y) = 1$ and the aspect ratio $\delta = 1.1$. Both the components relax toward zero, showing the asymptotic stability of the Euler equations.

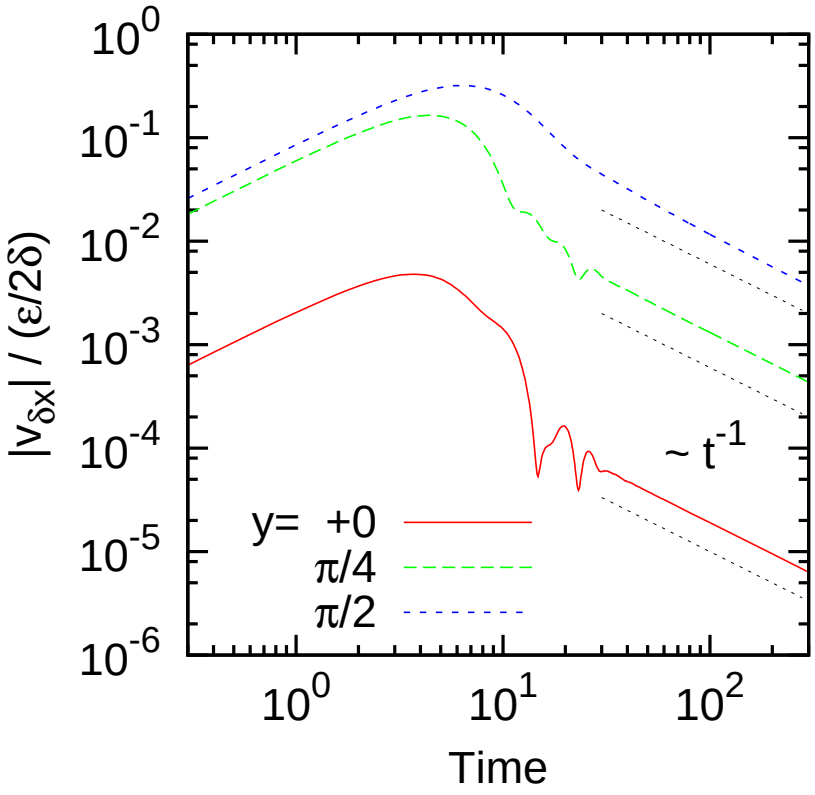

(a)

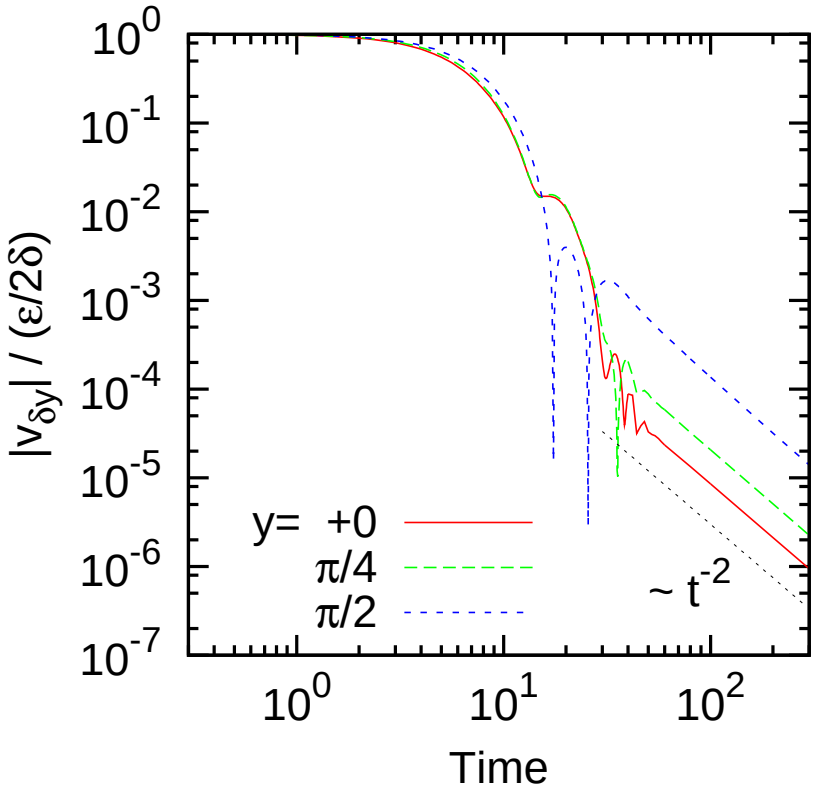

(b)

Figure 12: The time series of perturbation velocity components $|v_{\delta,x}(y,t)|$ (a) and $|v_{\delta,y}(y,t)|$ (b) at three locations, $y = 0$ (vicinity of the stationary streamline) (red), $y = \pi/4$ (green), and $y = \pi/2$ (blue), for the initial perturbation profile $A(y) = 1$ and the aspect ratio $\delta = 1.1$. We observe the asymptotic forms $|v_{\delta,x}(y,t)| \sim t^{-\alpha}$, with $\alpha = 1$, and $|v_{\delta,y}(y,t)| \sim t^{-\beta}$, with $\beta = 2$, in accordance with the theory for the asymptotic bahavior of the velocity (equations (35) and (36))

Asymptotic decay of the velocity perturbation for even perturbations. The space-time series of the modulus of the perturbation velocity components $|v_{\delta,x}(y,t)|$ and $|v_{\delta,y}(y,t)|$ are shown in Figure 11. The relaxation to zero of the velocity perturbation illustrates the asymptotic stability of the velocity for the 2D Euler dynamics.

We investigate the asymptotic behavior of the velocity perturbation more precisely. Figure 12 shows the time series at several y's. As shown, their asymptotic forms are $|v_{\delta x}(y,t)| \sim t^{-\alpha}$, with $\alpha = 1$, and $|v_{\delta y}(y,t)| \sim t^{-\beta}$, with $\beta = 2$. This is in agreement with the theoretical predictions for the asymptotic behavior of the velocity perturbation (see equations 35 and 36)).

Odd perturbations. Next, we consider initial perturbations where $A(y)$ has a parity opposite to the base flow velocity one's. In particular, we examine $A(y) = \sin y$.

The space-time series of $|\omega_\delta(y,t)|$ is shown in Figure 13. It shows an initial rapid relaxation toward the final profile, as expected from the theory (equation (34). Because the parity of the perturbation is conserved for all time, the vorticity profile remains odd. Then $|\omega_\delta(y,t)|$ is zero for $y = 0$ and $y = \pi$ (stationary streamlines), as expected.

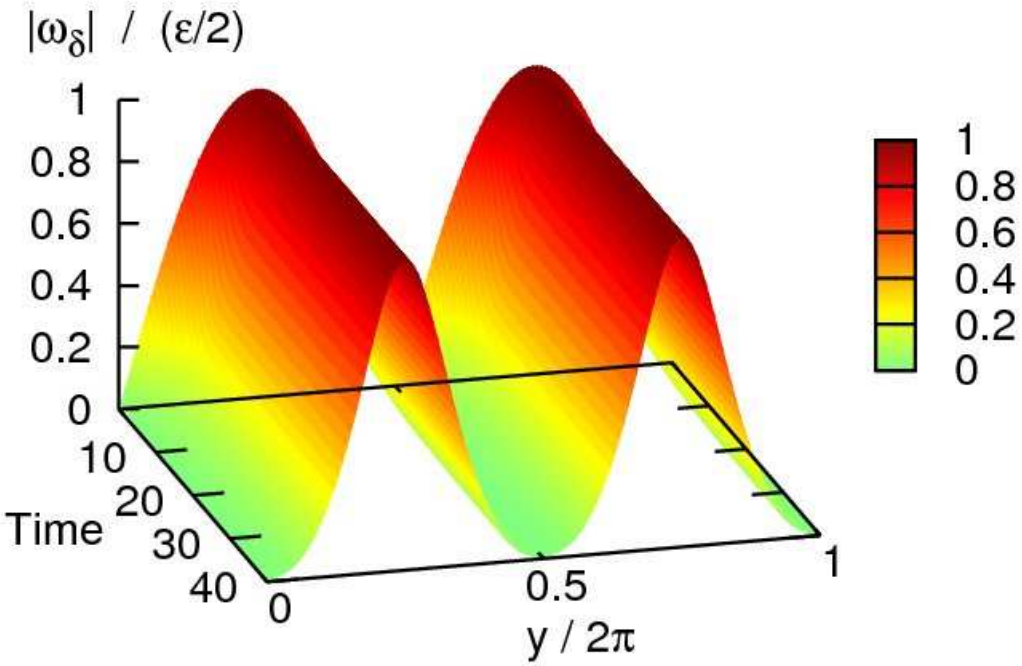

Figure 13: The space-time series of the modulus of the perturbation vorticity, $|\omega_\delta(y,t)|$, with initial perturbation profile $A(y) = \sin y$, and aspect ratio $\delta = 1.1$.

The rapid relaxation is again followed by an algebraic convergence to the final profile. In particular, in the vicinity of $y = 0$ and $y = \pi$ (stationary streamlines), it relaxes as slowly as, $t^{-1/2}$, in this case. The vorticity is always zero at the stationary streamlines, the profile in the vicinity is linear (see figure 14), an not flat as in the case of even perturbations. However, as time goes on, this linear region becomes narrower and narrower, and instead an outer region with profile locally propotional to $\sim y^2$ becomes wider. This indicates that, in the large time limit, the profile is locally parabolic in the vicinity of the stationary streamlines, as in the case of even perturbations. The profile beeing odd, we remark that such a parabolic profile means that the asymptotic vorticity profile is not twice differentiable at the stationary streamlines.

The final profile obtained from the Laplace transform tools (equation (34)) and the direct numerical simulations again show excellent agreement (see Figure 15).

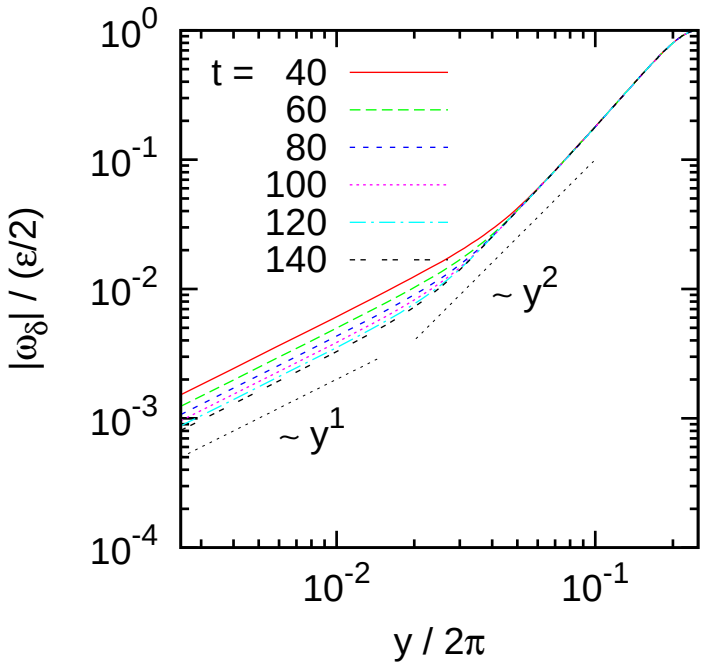

Figure 14: The profiles of the perturbation vorticity modulus, $|\omega_\delta(y,t)|$, at several times, for the initial perturbation profile $A(y) = \sin y$ and aspect ratio $\delta = 1.1$. As the time goes on, the linear region becomes narrower and narrower, and an outer region with $|\omega_\delta(y,t)| \sim y^2$ becomes wider and wider, indicating the parabolicity of the profile in the large time limit.

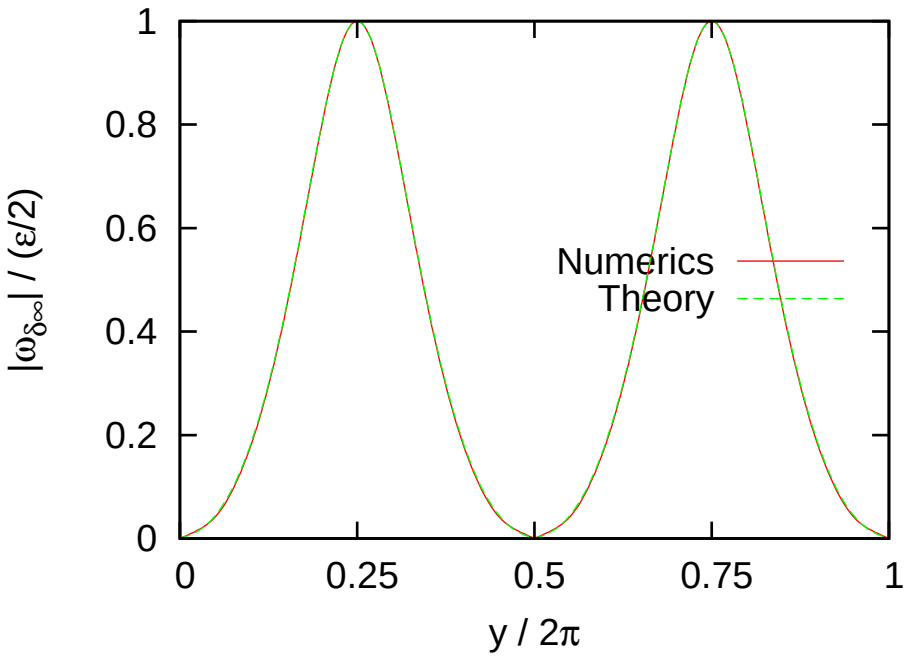

Figure 15: The final profile of the perturbation vorticity modulus, $|\omega_{\delta\infty}(y)|$, obtained from both numerics and theory. The initial perturbation profile is $A(y) = \sin y$ and the aspect ratio is $\delta = 1.1$. The two profiles show excellent agreement.

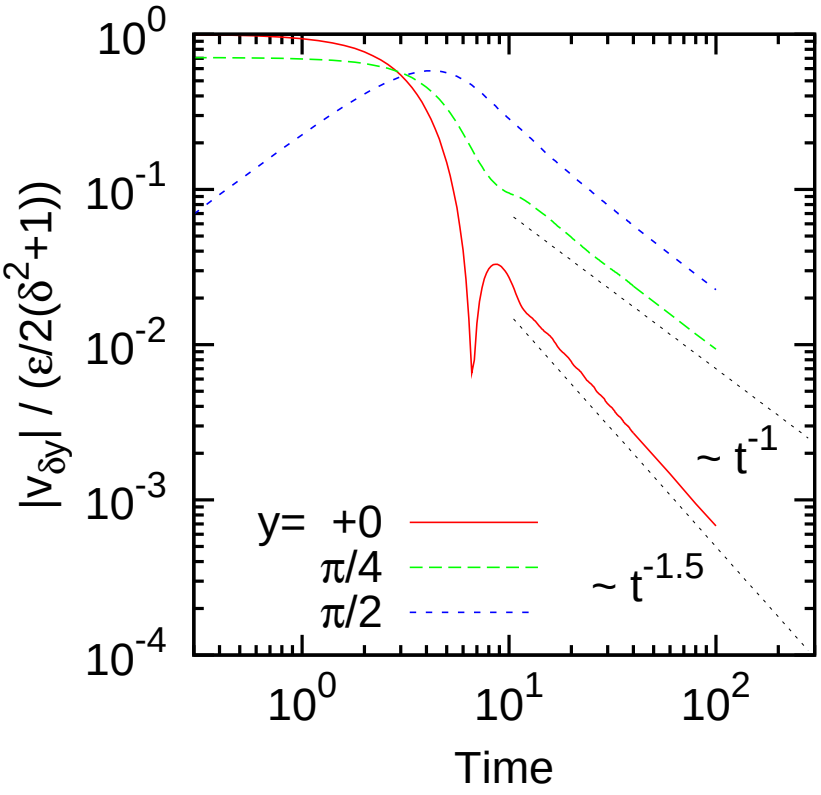

(a)

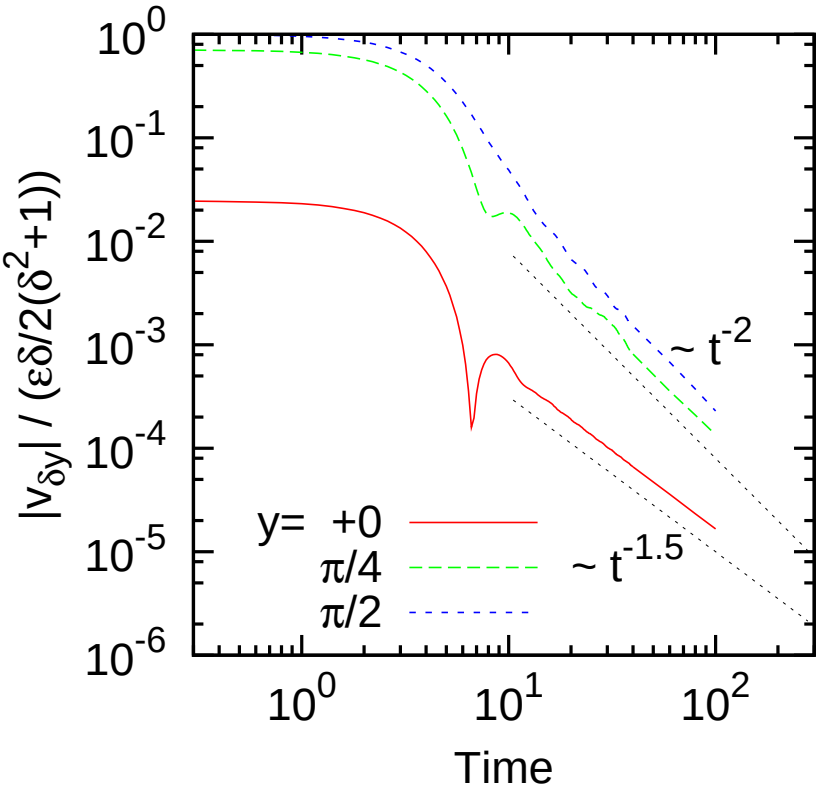

(b)

Figure 16: The time series of the perturbation velocity components, $|v_{\delta,x}(y,t)|$ (a) and $|v_{\delta,y}(y,t)|$ (b) at three locations, $y = 0$ (vicinity of the stationary streamline) (red), $y = \pi/4$ (green), and $y = \pi/2$ (blue), for the initial perturbation profile $A(y) = \sin y$ and aspect ratio $\delta = 1.1$. We observe the asymptotic forms $|v_{\delta,x}(y,t)| \sim t^{-\alpha}$, with $\alpha = 1$, and $|v_{\delta,y}(y,t)| \sim t^{-\beta}$, with $\beta = 2$, in the almost all the region, in accordance with the theory. Only in the vicinity of $y = 0$ and π, we observe the exponents $\alpha = 1.5$ and $\beta = 1.5$, for which we have no theoretical predictions.

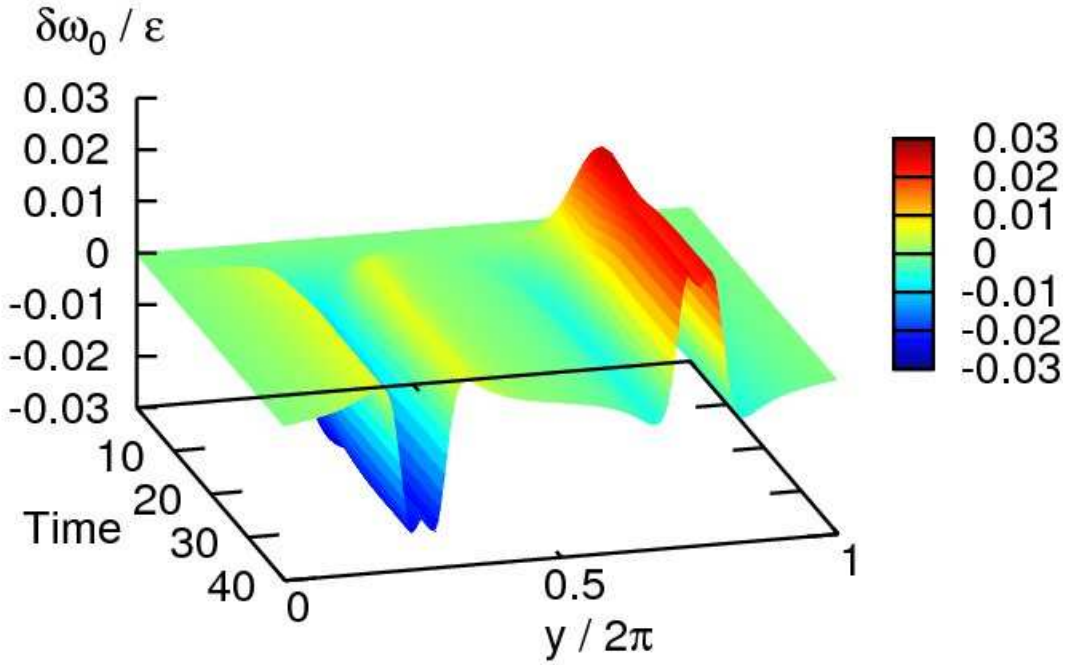

Figure 17: The space-time series of the x-averaged perturbation vorticity, $\delta\omega_0(y,t)$. The initial perturbation profile is $A(y) = 1$ and the aspect ratio is $\delta = 1.1$.

The space-time series of $|v_{\delta,x}(y,t)|$ and $|v_{\delta,y}(y,t)|$, similarly to the case of $A(y) = 1$, shows a relaxation toward zero, illustrating the asymptotic stability of the Euler equations.

We investigate the velocity asymptotic behavior more precisely. Figure 16 shows the time series at several y's. As shown, their asymptotic forms are $|v_{\delta x}(y,t)| \sim t^{-\alpha}$, with $\alpha = 1$, and $|v_{\delta y}(y,t)| \sim t^{-\beta}$, with $\beta = 2$, for almost all values of y. Only in the vicinity of $y = 0$ and π (stationary streamlines), the exponents are changed to $\alpha = 1.5$ and $\beta = 1.5$. We recall that we have no theoretical predictions for these special points. Thus we verify that the numerics for the asymptotic behavior of the velocity perturbation is in good agreement with the theory.

In the last paragraphs, we have compared, for the mode ω_δ, direct numerical simulations of the 2D Euler equations (nonlinear), with the predictions of the 2D linearized Euler equations. The agreement between both is extremely good. We actually see no differences at eye even for large times. This is in agreement with the theoretical discussion of section 3 ; differences are then expected to be of order ϵ^2. To summarize, we conclude that the results of the direct numerical simulations and the asymptotic behavior of the (nonlinear) Euler equations are very well described by the quasi-linear theory discussed in the previous sections.

Evolution of the base flow profile and asymptotic stability. We now consider the evolution of the base flow profile $\Omega_0(y,t)$ (the x-average vorticity, directly related to the x-average velocity, please see the discussion preceding equation (43) page 17)). We define the difference with respect to the initial profile by $\delta\omega_0(y,t) = \Omega_0(y,t) + U'(y)$. We thus have

$$\delta\omega_0(y,t) = \int \frac{\mathrm{d}x}{2\pi\delta^1}\omega(x,y,t). \tag{49}$$

The evolution of the base profile $\delta\omega_0(y,t)$ is due to nonlinear effects (see eq. (43) page 17). Figure 17 shows this evolution computed using direct numerical simulations. It illustrated that the perturbation vorticity converges extremely rapidly (on times of order $t = 15$ which correspond to the linear shear times) toward a fixed perturbation profile. The asymptotic perturbation profile is of order ϵ^2. All these are in agreement with the theoretical discussions of section 3.

5 Discussion

In this paper, we have discussed the asymptotic stability of parallel flows for the 2D Euler equations. Our results are valid for any flow that have no modes for the linearized dynamics (neither unstable nor neutral ones). This situation is a generic one, as the example of the Kolmogorov flows (section 4) illustrates. An adaptation of the present results to the case where the flow has neutral modes would be easy. Our results are valid for base flows $U(y)$ with or without stationary streamlines y_0 such that $U'(y_0) = 0$. We have emphasized the case with stationary streamlines that has not been studied before.

For the linearized Euler equation, we have proven that Lundgren's ansatz (2) actually describes the asymptotic vorticity field for large times. The asymptotic vorticity field thus oscillates, for each streamline, at the streamline frequency. The asymptotic vorticity profile depends both on the initial condition in a non trivial way, and on the base flow. The asymptotic vorticity is always strongly affected by the base flow structure, in a nonlocal way, especially when stationary streamlines exist. It is thus unlikely that a description based on the local shear give a good quantitative description, except may be in a limit or nearly linear shear. We have also shown that this asymptotic profile can be computed directly from the resolvent operator of the linearized Euler equation (see equation (34) and figure 10) without performing costly direct numerical computation of the Euler equations.

For the linearized Euler equation, we have also proven that the asymptotic velocity field decays algebraically for large times (equation 1), with exponents $\alpha = 1$ and $\beta = 2$ for any streamlines that are not stationary ($U'(y_0) = 0$). On the stationary streamlines, we have no theoretical predictions, but we have found numerically that two cases exist $\alpha = 1$ and $\beta = 2$ for perturbation vorticities having the same periodicity as the base flow velocity or $\alpha = 3/2$ and $\beta = 3/2$ for perturbation vorticities having the opposite periodicity with respect to the base flow. Without stationary streamlines, these results are the same as the classically expected ones. With stationary streamlines, they are unexpected as the effect of the stationary streamlines in oscillating integrals are expected to give $1/\sqrt{(t)}$ contributions. These cancel out because of a self-consistent vorticity depletion at the stationary streamline. This new mechanism of vorticity depletion at the stationary streamline that we theoretically predict and numerically confirm in this paper.

This vorticity depletion mechanism occurs due to the effects of the transverse component of the velocity perturbation on the background vorticity gradient. This mechanism is thus absent in cases where the background vorticity gradient identically vanishes, or for a beta-plane barotropic flow when the beta effect exactly balance the vorticity gradient, a case studied in several papers [15, 13]. We think that this last case is not generic as the vorticity depletion mechanism exists as soon as the vorticity gradient is not exactly balanced.

We use the above results to prove that if the perturbation evolves according to the linearized Euler equation, the nonlinear term remains uniformly bounded in time, and actually decays algebraically for large times. Based on these results, we argue that for the Euler equations (nonlinear), a quasilinear treatment of the nonlinear terms is self consistent. This strongly suggests that such a quasilinear treatment of the nonlinear term should be valid. This also suggests that the full nonlinear equation converges towards Lundgren's type asymptotics for the perturbation vorticity field and to zero for the asymptotic velocity field, extremely rapidly.

From these theoretical arguments, we then expect that the velocity of parallel flows without unstable or neutral linear modes is asymptotically stable : the velocity converges towards a new parallel flow which is very close to the initial one, even in the absence of dissipation. The distance between the initial profile and the asymptotic one is of order ϵ^2, where ϵ is the order of magnitude of the initial perturbation.

Direct numerical simulations of the Euler equations close to the Kolmogorov base flow show an excellent agreement with the above theoretical predictions.

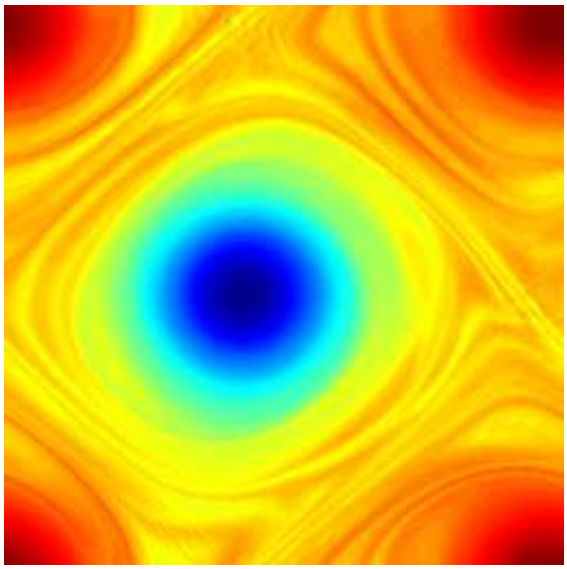

Figure 18: A snapshot of the vorticity field for the Navier-Stokes equation with stochastic forces, in a statistically stationary regime. The vorticity field is close to a steady state of the Euler equation (here a dipole). The fluctuations close to this state are the visible filaments on the figure. One clearly see that such filaments are present in between the two vortices, but are absent in the core of the vortices. This is due to the vorticity depletion mechanism at the core of the vortices, the points where the angular velocity of the vortices have local extrema.

The theoretical study performed in this paper, could be easily generalized to the study of the asymptotic behavior and stability of jets in the context of both barotropic flows in the beta-plane approximations, or two dimensional axisymmetric vortices. Many recent works have considered perturbations to two dimensional vortices [58, 3, 6, 47, 49]. As far as asymptotic behavior is concerned, following this paper approach, in the case of vortices, we argue that a similar perturbation vorticity depletion should occur at any stationary point of the angular velocity of the vortex $U(r)/r$. For instance in the case of a monotonic angular velocity, such a stationary point of the angular velocity is located at the core of the vortex $r = 0$, and the vorticity depletion occurs at the center of the vortex. This phenomena has indeed been observed by Bassom and Gilbert [7] (see their discussion, and the comment of their figure 2(b) and 4(a)). They have stated that "We at present lack a simple physical explanation of this process whereby vorticity is more highly suppressed than a passive scalar, and do not know whether it has applicability beyond the Gaussian vortex". The type of arguments developed in the present paper, based on the Laplace tools, suggests that such a vorticity depletion is indeed a generic

phenomenon, valid for any parallel flow (resp. circular vortex), at the stationary points of the velocity profile (resp. angular velocity profile). Mathematically this is due to the regularization of the critical layer singularities at the edge of the continuous spectrum.

This vorticity depletion mechanism also impacts turbulent flows where the perturbations are locally governed by the linearized equations. Fig 18 shows a snapshot of the vorticity field in the dynamics of the stochastic 2D Navier-Stokes equations [10]. One clearly observes a depletion of the vorticity fluctuations at the core of the vortices. This effect in a stochastically forced equation is related to the depletion mechanism in a deterministic equation, described in this paper.

We have treated the linearized dynamics and the asymptotic stability for the case of parallel flows, for the 2D Euler dynamics. The generalization of such results for more complex cases, for instance flow with separatrix and stationary points would also be extremely interesting. The problem is then much more difficult from a theoretical point of view, but could be addressed numerically. Also the time dependent situation, by contrast to the case of perturbation of steady base flows, is of a large interest. It has been shown numerically that interactions with large scales dominate the small scale dynamics [22, 32], in the spirit of rapid distortion theory or quasilinear approaches. This has deep impact on the statistics of the associated turbulence [39].

Because both are transport equations by a nondivergent field, there is a very well known analogy between the Vlasov equations and the 2D Euler equations. Both equations have very similar behaviors, including for instance relaxations without dissipation (Orr mechanism or Landau damping) and the associated asymptotic stability. The theory of the asymptotic stability of 2D Euler equations is thus deeply related to the asymptotic stability of Vlasov equations. We note very recent mathematical results on nonlinear Landau damping [38], a subject related to the asymptotic stability of Vlasov equations. A natural issue, is to know if such recent mathematical results [38], could be generalized to the case of the 2D Euler equations, in relations with the results obtained in the present work.

The current work has interesting consequences for the understanding of the linearized Euler and Navier Stokes equations with stochastic forces, and of the Euler and Navier Stokes equations with stochastic forces when the large scale stuctures dominate the dynamics. This was one of our motivation for studying the asymptotic behavior of the linearized Euler equation and asymptotic stability of the Euler equations. These consequences will be developed in a forthcoming work.

Acknowledgments

We warmly thank J. Barré and E. Simonnet for usefull discussions about this work.

This work was supported by the ANR program STATFLOW (ANR-06-JCJC-0037-01).

A) Oscillating integrals

A-1) General classical results

Let us consider the asymptotic behavior, for large t, of the integral

$$I(t) = \int_a^b dx\, g(x) \exp(if(x)t) \tag{50}$$

1. We here suppose that f and g are twice differentiable and that f has no singular points : for any x, $f'(x) \neq 0$, and that either $g(a) \neq 0$ or $g(b) \neq 0$. Then

$$I(t) \sim \frac{1}{it}\left[\frac{g(b)\exp(itf(b))}{f'(b)} - \frac{g(a)\exp(itf(a))}{f'(a)}\right] \tag{51}$$

   This can be easily proved by part integrations. If $g(a) = g(b) = 0$ and if g and f are sufficiently differentiable, then the asymptotic behavior can be obtained by further part integrations.

2. We now suppose that f is a real function, with a single stationary point x_0 ($f'(x_0) = 0$). The asymptotic behavior of the oscillating integral (50) is then given by the classical stationary phase results [24, 8]. We suppose that f and g are smooth and that $f''(x_0) \neq 0$. Then

$$\int_a^b dx\, g(x) \exp(if(x)t) \underset{t\to\infty}{\sim} g(x_0)\sqrt{\frac{2\pi}{|f''(x_0)|}} \exp\left(\frac{i\epsilon\pi}{4}\right) \frac{\exp(itf(x_0))}{\sqrt{t}}, \tag{52}$$

   where ϵ is the sign of $f''(x_0)$

A-2) Oscillating integrals and the velocity asymptotic expansion

We apply the general methods of oscillating integrals to the particular case of the computation of the velocity from an oscillating vorticity field, like for instance the case given by equation (38). We first evaluate the long time asymptotics of

$$\mathbf{v}(y,t) = \int dy'\, \mathbf{G}_k(y,y') h(y') \exp(-ikU(y')t), \tag{53}$$

where the function h is assumed to be twice differentiable and where $\mathbf{G}_k$ is the Green function for the computation of the velocity $\mathbf{v}(y)\exp(ikx)$ from a vorticity field $\omega(y)\exp(ikx)$. We treat explicitly the case of a channel $-L < y < L$. The results are also valid for periodic boundary conditions for y, just by dropping all the contributions from the boundary in the expressions bellow.

We note that an explicit expression for $\mathbf{v}_k(y,t)$ can be computed when $v_0(y) = sy$ and when $h(y)$ is either a constant, a sine (cosine) or a sinh (cosh) (see [17]). Clearly, (53) is an oscillating integral. In order to study its asymptotic expansion, we use the results of section A-1 of this appendix.

Let us first treat the case without stationary point. We use that $\mathbf{G}_k(y,.)$ is smooth everywhere, except for $y' = y$ (see appendix B). Then we can use results on asymptotic behaviors of oscillating integrals (section A-1) for both intervals $-L < y' < y$ and $y < y' < L$ independently. We assume that $h(y)$ is at least twice differentiable. We then obtain that

$$v_x(y,t) \underset{t\gg l/ks}{\sim} -\frac{1}{ikst}\left[G_{k,x}(y,L)\,h(L)\exp(-ikU(L)t) - G_{k,x}(y,-L)\,h(-L)\exp(ikU(-L)t) + h(y)\exp(-ikU(y)t)\right]; \tag{54}$$

the first two terms are contributions from the boundaries and the third term is due to the discontinuity of $G_{k,x}(y,y')$ for $y = y'$ (see (58) in appendix B). Here we define s as the minimum shear rate $s = \min(U'(y))$, and l is a typical length scale, that characterizes the variations of $h(y)$. Similarly we obtain

$$v_y(y,t) \underset{t\gg l/ks}{\sim} \frac{1}{k^2s^2t^2}\left[\frac{\partial G_{k,y}}{\partial y'}(y,L)\,h(L)\exp(-ikU(L)t) - \frac{\partial G_{k,y}}{\partial y'}(y,-L)\,h(-L)\exp(ikU(L)t) - ikh(y)\exp(-ikU(y)t)\right] \tag{55}$$

We note that there is no contribution of order $1/t$ in this case, because G_k vanishes at the boundaries ($G_{k,y}(y,L) = 0$, see (59) in appendix B) and because $G_{k,y}(y,y')$ has a discontinuity of its first derivative

only, for $y' = y$ (see (60) in appendix B).

We now treat the case of a base flow with stationary points y_m such that $U'(y_m) = 0$. We assume that each stationary point y_m is not degenerated ($f''(y_m) \neq 0$). We perform the computation for one of these, denoted y_0. The general result then follows.

The classical results on oscillating integrals (52), assume that the function g (see Eq. 50) is smooth. This is not always the case for us, actually the Green function $G_k(y, y')$ is not smooth for $y = y'$. If $y \neq y_0$, this discontinuity for G_k or for its derivative, can easily be handled by dividing the integration interval in two subintervals, as has been done in the previous paragraph. Then one concludes that the leading order of the asymptotic behavior is still dominated by the contribution of the stationary points. Thus the result (52) is still valid.

Then, from (53), using (52), we obtain that for $y \neq y_0$

$$\mathbf{v}(y,t) \underset{t\to\infty}{\sim} \mathbf{G}_k(y, y_0)h(y_0)\sqrt{\frac{2\pi}{|kU''(y_0)|}}\exp\left(\frac{i\epsilon_k\pi}{4}\right)\frac{\exp(-ikU(y_0)\,t)}{\sqrt{t}}, \tag{56}$$

where ϵ_k is the sign of $-kU''(y_0)$. We note that the asymptotic expansion has a discontinuity for $y = y_0$, due to the discontinuity of the Green function. A straightforward generalization of the classical results (52), to oscillating integrals with discontinuous functions g, allows to conclude that this discontinuity is regularized over a length scale $l = \sqrt{1/(|kU''(y_0)|\,t)}$, that decreases with time.

B) Green functions

Let us establish the expression and some properties for the velocity Green function $\mathbf{G}_k$. The results on the discontinuity of the Green function, equations (58) and (60) bellow, are necessary for the discussion of appendix A. We treat the case of a channel geometry $-L \leq y \leq L$, but the case of periodic boundary conditions could be treated similarly and equations (58) and (60) would remain unchanged in that case.

Let us denote H_k the Green function for the stream function. Starting from $\omega = \Delta\psi$, we obtain that the Fourier transforms in the x direction verify $\omega_k = d^2\psi_k/dy^2 - k^2\psi_k$. $H_k(y, y')$ is thus solution of

$$\frac{\partial^2 H_k}{\partial y^2} - k^2 H_k = \delta(y - y') \tag{57}$$

with the boundary conditions $H_k(L, y') = 0$ and $H_k(-L, y') = 0$.

We note that $H_k(y, y')$, considered as function of y, is smooth everywhere except for $y = y'$. For $y = y'$, H_k is differentiable and has a jump unity for its first derivative :

$$\frac{\partial H_k}{\partial y}(y'^+, y') - \frac{\partial H_k}{\partial y}(y'^-, y') = 1,$$

where $F(y'^+, y')$ his the limit of $F(y, y')$ for y' going to y with the condition $y > y'$.

When $y' = L$, we have for all y, $d^2H_k/dy^2 - k^2H_k = 0$ with $H_k(L, L) = 0$ and $H_k(-L, L) = 0$. Thus for all y

$$H_k(y, L) = H_k(L, y)$$

Besides these general properties, an explicit expression to H_k can be found from (57) :

$$\text{for } y > y' \;\; H_k(y, y') = \frac{\sinh(k(y' + L))\sinh(k(y - L))}{k\sinh(2kL)} \text{ and}$$

$$\text{for } y < y' \;\; H_k(y, y') = \frac{\sinh(k(y' - L))\sinh(k(y + L))}{k\sinh(2kL)} \text{ and}$$

By direct computation, one can verify that $H_k(y, y')$, considered as a function of y', is differentiable and has a discontinuity in its derivative for $y' = y$. By direct computation, we have

$$\frac{\partial H_k}{\partial y}(y, y^+) - \frac{\partial H_k}{\partial y}(y, y^-) = 1$$

Then using $\mathbf{v} = \nabla \wedge (\psi \mathbf{e}_z)$, we have for the Fourier transforms : $\mathbf{v}_{k,x} = -d\psi_k/dy$ and $\mathbf{v}_{k,y} = ik\psi_k$. Thus

$$\mathbf{G}_k = \left(-\frac{\partial H_k}{\partial y}, ikH_k \right)$$

Then, using the properties of H_k, we note that $\mathbf{G}_k(., y')$ is smooth everywhere except for $y = y'$, that its derivative has a jump for $y = y'$. We have

$$\mathbf{G}_k\left(y, y^+\right) - \mathbf{G}_k\left(y, y^-\right) = (-1, 0) \tag{58}$$

$$\mathbf{G}_k(y, L) = \left(\frac{\sinh(k(y+L))}{\sinh(2kL)}, 0 \right) \text{ and } \mathbf{G}_k(y, -L) = \left(\frac{\sinh(k(y-L))}{\sinh(2kL)}, 0 \right) \tag{59}$$

and

$$\frac{\partial \mathbf{G}_{k,y}}{\partial y}\left(y, y^+\right) - \frac{\partial \mathbf{G}_{k,y}}{\partial y}\left(y, y^-\right) = ik \tag{60}$$

$$\frac{\partial \mathbf{G}_{k,y}}{\partial y}(y, L) = -\frac{ik\sinh(k(y+L))}{\sinh(2kL)} \text{ and } \frac{\partial \mathbf{G}_{k,y}}{\partial y}(y, -L) = -\frac{ik\sinh(k(y-L))}{\sinh(2kL)}$$

References

[1] A. Antkowiak and P. Brancher. Transient energy growth for the Lamb-Oseen vortex. *Physics of Fluids*, 16:L1–L4, January 2004.

[2] V. I. Arnold. On an a-priori estimate in the theory of hydrodynamic stability. *Izv. Vyssh. Uchebbn. Zaved. Matematika; Engl. transl.: Am. Math. Soc. Trans.*, 79(2):267–269, 1966.

[3] K. Bajer, A. P. Bassom, and A. D. Gilbert. Accelerated diffusion in the centre of a vortex. *Journal of Fluid Mechanics*, 437:395–411, June 2001.

[4] N. J. Balmforth and P. J. Morrison. A necessary and sufficient instability condition for inviscid shear flow. *ArXiv Physics e-prints*, September 1998.

[5] N. J. Balmforth and P. J. Morrison. A necessary and sufficient instability condition for inviscid shear flow. *Studies in Appl. Math.*, 102:309–344, 1999.

[6] N. J. Balmforth, S. L. Smith, and W. R. Young. Disturbing vortices. *APS Meeting Abstracts*, pages 4–+, November 1999.

[7] A. P. Bassom and A. D. Gilbert. The spiral wind-up of vorticity in an inviscid planar vortex. *Journal of Fluid Mechanics*, 371:109–140, September 1998.

[8] N. Bleistein and R. Handelsman. *Asymptotic Expansions of Integrals*. Dover, New York, 1975.

[9] F. Bouchet. Simpler variational problems for statistical equilibria of the 2D Euler equation and other systems with long range interactions. *Physica D Nonlinear Phenomena*, 237:1976–1981, August 2008.

[10] F. Bouchet and E. Simonnet. Random changes of flow topology in two dimensional and geophysical turbulence. *ArXiv e-prints*, 2008.

[11] R. J. Briggs, J. D. Daugherty, and R. H. Levy. Role of Landau Damping in Crossed-Field Electron Beams and Inviscid Shear Flow. *Physics of Fluids*, 13:421–432, February 1970.

[12] S. N. Brown and K. Stewartson. On the algebraic decay of disturbances in a stratified linear shear flow. *Journal of Fluid Mechanics*, 100:811–816, 1980.

[13] G. Brunet and P. H. Haynes. The Nonlinear Evolution of Disturbances to a Parabolic Jet. *Journal of Atmospheric Sciences*, 52:464–477, February 1995.

[14] G. Brunet and M. T. Montgomery. Vortex Rossby waves on smooth circular vortices - Part I. Theory. *Dynamics of Atmospheres and Oceans*, 35:153–177, May 2002.

[15] G. Brunet and T. Warn. Rossby Wave Critical Layers on a Jet. *Journal of Atmospheric Sciences*, 47:1173–1178, May 1990.

[16] E. Caglioti, M. Pulvirenti, and F. Rousset. The 2D constrained Navier Stokes equation and intermediate asymptotics. *Journal of Physics A Mathematical General*, 41:H4001+, August 2008.

[17] K. M. Case. Stability of Inviscid Plane Couette Flow. *Physics of Fluids*, 3:143–148, March 1960.

[18] P.H. Chavanis. Statistical mechanis of two-dimensional vortices and stellar systems. In T. Dauxois, S. Ruffo, E. Arimondo, and M. Wilkens, editors, *Dynamics and Thermodynamics of Systems With Long Range Interactions*, 2002.

[19] L. A. Dikii. The Stability of Plane-Parallel Flows of an Ideal Fluid. *Soviet Physics Doklady*, 5:1179, 1960.

[20] P. G. Drazin and W. H. Reid. *Hydrodynamic stability*. Cambridge university press, 2004, second edition.

[21] D. H. E. Dubin and T. M. O'Neil. Two-dimensional guiding-center transport of a pure electron plasma. *Phys. Rev. Lett.*, 60(13):1286–1289, Mar 1988.

[22] B. Dubrulle and S. Nazarenko. Interaction of turbulence and large-scale vortices in incompressible 2D fluids. *Physica D*, 110:123–138, 1997.

[23] R. S. Ellis, K. Haven, and B. Turkington. Nonequivalent statistical equilibrium ensembles and refined stability theorems for most probable flows . *Nonlinearity*, 15:239–255, March 2002.

[24] A. Erdélyi. *Asymptotic expansions*. Dover, New York, 1956.

[25] G. Eyink, U. Frisch, R. Moreau, and A. Sobolevski. *Euler: 250 years on*, volume 237 of *Physica D*. 2008.

[26] B. Farrell. Developing Disturbances in Shear. *Journal of Atmospheric Sciences*, 44:2191–2199, August 1987.

[27] B. F. Farrell and P. J. Ioannou. Generalized Stability Theory. Part I: Autonomous Operators. *Journal of Atmospheric Sciences*, 53:2025–2040, July 1996.

[28] B. F. Farrell and P. J. Ioannou. Structural Stability of Turbulent Jets. *Journal of Atmospheric Sciences*, 60:2101–2118, September 2003.

[29] S. Friedlander and L. Howard. Instability in Parallel Flows Revisited. *Studies in Applied Mathematics*, 101(1):1–21, 1998.

[30] E. Grenier, C. K. R. T. Jones, F. Rousset, and B. Sandstede. Viscous perturbations of marginally stable Euler flow and finite-time Melnikov theory. *Nonlinearity*, 18:465–483, March 2005.

[31] M. B. Isichenko. Nonlinear Landau Damping in Collisionless Plasma and Inviscid Fluid. *Physical Review Letters*, 78:2369–2372, March 1997.

[32] J.-P. Laval, B. Dubrulle, and S. V. Nazarenko. Fast numerical simulations of 2D turbulence using a dynamic model for subfilter motions. *J. Comp. Phys.*, 196:184–207, 2004.

[33] S. Le Dizès. Non-axisymmetric vortices in two-dimensional flows. *Journal of Fluid Mechanics*, 406:175–198, March 2000.

[34] T. S. Lundgren. Strained spiral vortex model for turbulent fine structure. *Physics of Fluids*, 25:2193–2203, December 1982.

[35] S. R. Maassen, H. J. H. Clercx, and G. J. F. van Heijst. Self-organization of decaying quasi-two-dimensional turbulence in stratified fluid in rectangular containers. *J. Fluid Mech.*, 495:19–33, 2003.

[36] D. Marteau, O. Cardoso, and P. Tabeling. Equilibrium states of two-dimensional turbulence: An experimental study. *Phys. Rev. E*, 51:5124–5127, 1995.

[37] Jonathan Miller. Statistical mechanics of euler equations in two dimensions. *Phys. Rev. Lett.*, 65(17):2137–2140, Oct 1990.

[38] C. Mouhot and C. Villani. On the Landau damping. *arXiv 0904.2760*.

[39] S. Nazarenko and J.-P. Laval. Non-local two-dimensional turbulence and Batchelor's regime for passive scalars. *J. Fluid Mech.*, 408:301–321, 2000.

[40] D. Nicholson. *Introduction to plasma theory*. Wiley, New-York, 1983.

[41] D. S. Nolan and M. T. Montgomery. The Algebraic Growth of Wavenumber One Disturbances in Hurricane-like Vortices. *Journal of Atmospheric Sciences*, 57:3514–3538, November 2000.

[42] W. M. F. Orr. The stability or instability of the steady motions of a perfect liquid and of a viscous liquid. *Proc. Roy. Irish Acad*, pages 9–69, 1907.

[43] J. Paret and P. Tabeling. Intermittency in the two-dimensional inverse cascade of energy: Experimental observations. *Phys. Fluids*, 10:3126–3136, 1998.

[44] L. Rayleigh. On the instability of jets. *Proc. Lond. Math. Soc*, 10:4–13, 1879.

[45] R. Robert. A maximum-entropy principle for two-dimensional perfect fluid dynamics. *J. Stat. Phys.*, 65:531–553, 1991.

[46] S. I. Rosencrans and D. H. Sattinger. On the spectrum of an operator occuring in the theory of hydrodynamic stability. *J. Math. Phys.*, 45:289–300, 1966.

[47] D. A. Schecter, D. H. E. Dubin, A. C. Cass, C. F. Driscoll, I. M. Lansky, and T. M. O'Neil. Inviscid damping of asymmetries on a two-dimensional vortex. *Physics of Fluids*, 12:2397–2412, October 2000.

[48] D. A. Schecter, D. H. E. Dubin, K. S. Fine, and C. F. Driscoll. Vortex crystals from 2D Euler flow: Experiment and simulation. *Phys. Fluids*, 11:905–914, 1999.

[49] D. A. Schecter and M. T. Montgomery. On the symmetrization rate of an intense geophysical vortex. *Dynamics of Atmospheres and Oceans*, 37:55–88, June 2003.

[50] K. Schneider and M. Farge. Final states of decaying 2D turbulence in bounded domains: influence of the geometry. *Physica D*, 2008.

[51] Roman Shvydkoy and Susan Friedlander. On recent developments in the spectral problem for the linearized euler equation. In Gui-Qiang Chen, George Gasper, and Joseph Jerome, editors, *Nonlinear partial differential equations and related analysis*, volume 371 of *Contemporary Mathematics*, pages 271–295. American Mathematical Society, 2005.

[52] E. Simonnet. On the unstable discrete spectrum of the linearized 2-D Euler equations in bounded domains. *Physica D Nonlinear Phenomena*, 237(20):2539–2552, October 2008.

[53] R. A. Smith and M. N. Rosenbluth. Algebraic instability of hollow electron columns and cylindrical vortices. *Physical Review Letters*, 64:649–652, February 1990.

[54] A. Sommerfeld. Ein beitrag zur hydrodynamischen erklaerung der turbulenten fluessigkeitsbewegungen. *Proceedings 4th International Congress of Mathematicians, Rome*, 3:116–124, 1908.

[55] J. Sommeria. Experimental study of the two dimensional inverse energy cascade in a square box. *J. Fluid. Mech.*, 170:139–168, 1986.

[56] W. Thomson. Rectilinear motion of viscous fluid between two parallel plates. *Philos. Mag.*, 24:188–196, 1887.

[57] K. K. Tung. Initial-value problems for Rossby waves in a shear flow with critical level. *Journal of Fluid Mechanics*, 133:443–469, August 1983.

[58] M. R. Turner and A. D. Gilbert. Linear and nonlinear decay of cat's eyes in two-dimensional vortices, and the link to Landau poles. *J. Fluid Mech.*, 593:255–279, 2007.

[59] F. Volponi. Local algebraic instability of shear-flows in the Rayleigh equation. *Journal of Physics A Mathematical General*, 38:4293–4307, May 2005.

[60] G. Wolansky and M. Ghil. Nonlinear Stability for Saddle Solutions of Ideal Flows and Symmetry Breaking. *Commun. Math. Phys.*, 193:713–736, 1998.

[61] T. Yamagata. On trajectories of Rossby wave-packets released in a lateral shear flow. *Journal of Oceanography*, 32:162–168, 1976.